


Review

Colchicine-Binding Site Inhibitors from Chemistry to Clinic: A Review

Eavan C. McLoughlin * and Niamh M. O'Boyle 

School of Pharmacy and Pharmaceutical Sciences, Trinity Biomedical Sciences Institute, Trinity College Dublin, D02 Dublin, Ireland; niamh.oboyle@tcd.ie

* Correspondence: mclougea@tcd.ie; Tel.: +353-1-896-2809

Received: 29 November 2019; Accepted: 23 December 2019; Published: 3 January 2020



Abstract: It is over 50 years since the discovery of microtubules, and they have become one of the most important drug targets for anti-cancer therapies. Microtubules are predominantly composed of the protein tubulin, which contains a number of different binding sites for small-molecule drugs. There is continued interest in drug development for compounds targeting the colchicine-binding site of tubulin, termed colchicine-binding site inhibitors (CBSIs). This review highlights CBSIs discovered through diverse sources: from natural compounds, rational design, serendipitously and via high-throughput screening. We provide an update on CBSIs reported in the past three years and discuss the clinical status of CBSIs. It is likely that efforts will continue to develop CBSIs for a diverse set of cancers, and this review provides a timely update on recent developments.

Keywords: anti-cancer; anti-tubulin; tubulin binding; microtubule-targeting agents; colchicine; colchicine binding site; combretastatin; CA-4; tubulin destabilizing

1. Microtubules as a Target for Treating Cancer

Microtubules are major components of the eukaryotic cytoskeleton conserved across evolution. They are involved in cellular motility, intracellular transport, cell structure and maintenance of cell structure. Most importantly, in the context of anti-cancer small-molecule drug development, microtubules are responsible for the separation of chromosomes during mitosis [1]. Mitosis is the fifth phase of a typical cell cycle in which DNA is divided into two daughter cells. Mitosis is an important target for anti-cancer agents due to loss of normal cell cycle controls in malignant cells. Cancer cell hallmarks include alterations which result in unscheduled and uncontrolled proliferation in addition to genomic instability. Numerous anti-cancer strategies have focused on targeting the rapid multiplication of cancer cells in order to arrest the cell cycle and specifically kill cancer cells [2].

Microtubules are described as 'dynamic polymers' and are composed of tubulin heterodimers formed from α and β tubulin monomers. Tubulin is a globular protein that exists as an $\alpha\beta$ heterodimer and is the principle building block of microtubule structures. α and β Tubulin are both 50 kDa in size and share 40% identity in amino acid homology.

Each microtubule consists of α and β tubulin heterodimers assembled together, associating in head-to-tail format to make linear protofilaments. Thirteen protofilaments associate laterally and wind together to form a 24 nm diameter, long, hollow cylinder known as the microtubule: a polar structure with a "+ end" (fast growing) and a "- end" (slow growing) (Figure 1) [3].

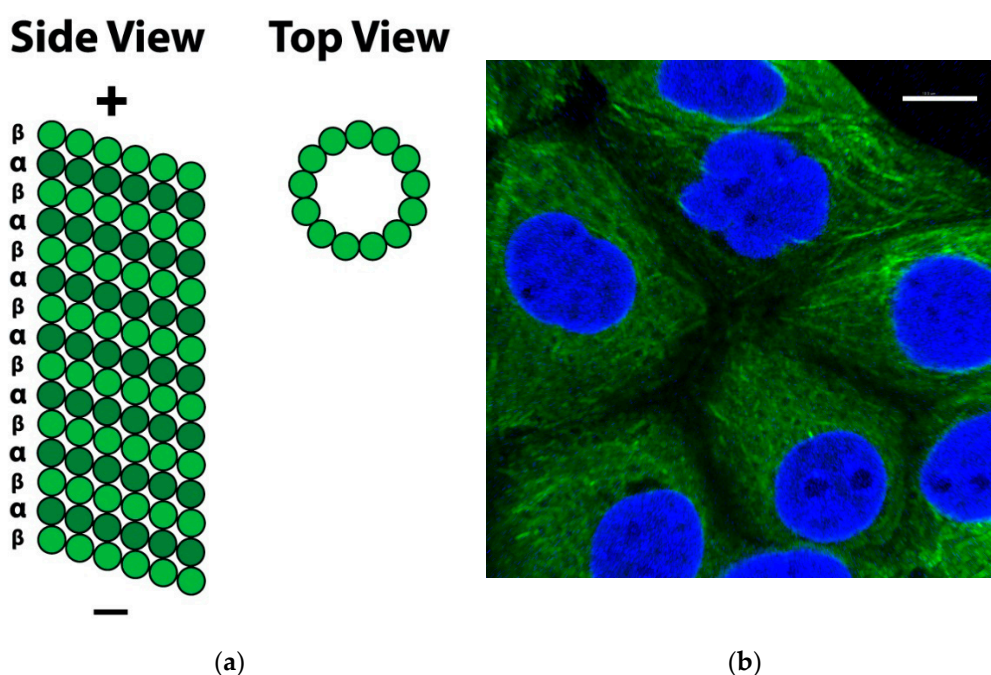


Figure 1. Microtubule structure from side and top perspectives. (a): Side View: Long, linear protofilaments consisting of $\alpha\beta$ -tubulin heterodimers associate laterally; Top View: Association of 13 protofilaments forms the microtubule, a long hollow cylinder. (b): Microtubule network in MCF-7 breast cancer cells. Cells were stained with mouse monoclonal anti- α -tubulin–fluorescein isothiocyanate (FITC) antibody (clone DM1A) (tubulin, green) and Alexa Fluor 488 dye, then counterstained with 4',6-diamidino-2-phenylindole (DAPI) (nuclei, blue). Scale bar: 10 μ M.

Microtubules alternate between periods of growth and shrinkage in what is known as ‘dynamic instability’. This occurs through the addition of guanosine triphosphate (GTP)-bound tubulin at the positive pole and the removal of guanosine diphosphate (GDP)-bound tubulin at the negative pole. Tubulin heterodimers bind GTP reversibly at the β -subunit. GTP is hydrolysed to GDP during polymerisation, which leads to loss of a GTP cap. Microtubules also undergo periods of polymerisation and depolymerisation, continually assembling and disassembling inside the cell. The phase of polymerisation versus depolymerisation is determined by the rate of the addition of GTP-bound tubulin. β -Tubulin binds GTP and in doing so regulates the rate of polymerisation of heterotubulin heterodimers. GTP hydrolysis to GDP weakens tubulin’s binding affinity for adjacent tubulin molecules and favours depolymerisation of microtubule structures. As long as GTP-bound tubulin units are added more rapidly than GTP is hydrolysed to GDP, a GTP cap at the positive pole is retained and microtubules will continue to grow. If the rate of GTP-bound tubulin slows, GTP at the “+ end” is hydrolysed, resulting in microtubule catastrophe and rapid depolymerisation [4].

The dynamics of microtubules in chemical equilibrium between an intracellular pool of $\alpha\beta$ -heterodimers and large microtubule polymers are tightly regulated and central to their biological functions. In dividing cells undergoing mitosis, the function of the microtubule is to form a mitotic spindle. When cells enter mitosis, the rate of microtubule growing and shortening increases up to 100-fold. This makes such cellular structures attractive targets for chemotherapy and anti-cancer drug development. These rapid dynamics are highly sensitive towards modulation by antimetabolic agents [5]. The majority of microtubule-binding agents (MTAs) bind to β -tubulin in the $\alpha\beta$ heterodimer and suppress microtubule dynamics. This causes a delay or blockade at the metaphase-anaphase transition during mitosis [5]. Due to the disruption at the mitotic spindle, spindle cell assembly check points are disrupted, causing extended mitotic arrest and cell death [6].

Microtubules are the targets of chemically diverse MTAs which have been used with great success in the treatment of cancer. Drugs that disrupt microtubule dynamics are widely used in

cancer chemotherapy. The vast majority act by binding to tubulin. MTAs both perturb mitosis and arrest cells during G₂/M phase of the cell cycle. MTAs interact with tubulin at a number of different binding sites: the laulimalide, maytansine, taxane/epothilone, vinca alkaloid and colchicine sites (Figure 2) [7]. Such agents are broadly categorised into two groups when used in high concentrations: microtubule-stabilizing agents including the taxanes, epothilones, and laulimalide and microtubule-destabilising agents inclusive of colchicine, the vinca alkaloids, and maytansine. This review will focus solely on microtubule-destabilising agents binding to the colchicine-binding site (CBS) of tubulin, termed colchicine-binding site inhibitors (CBSIs).

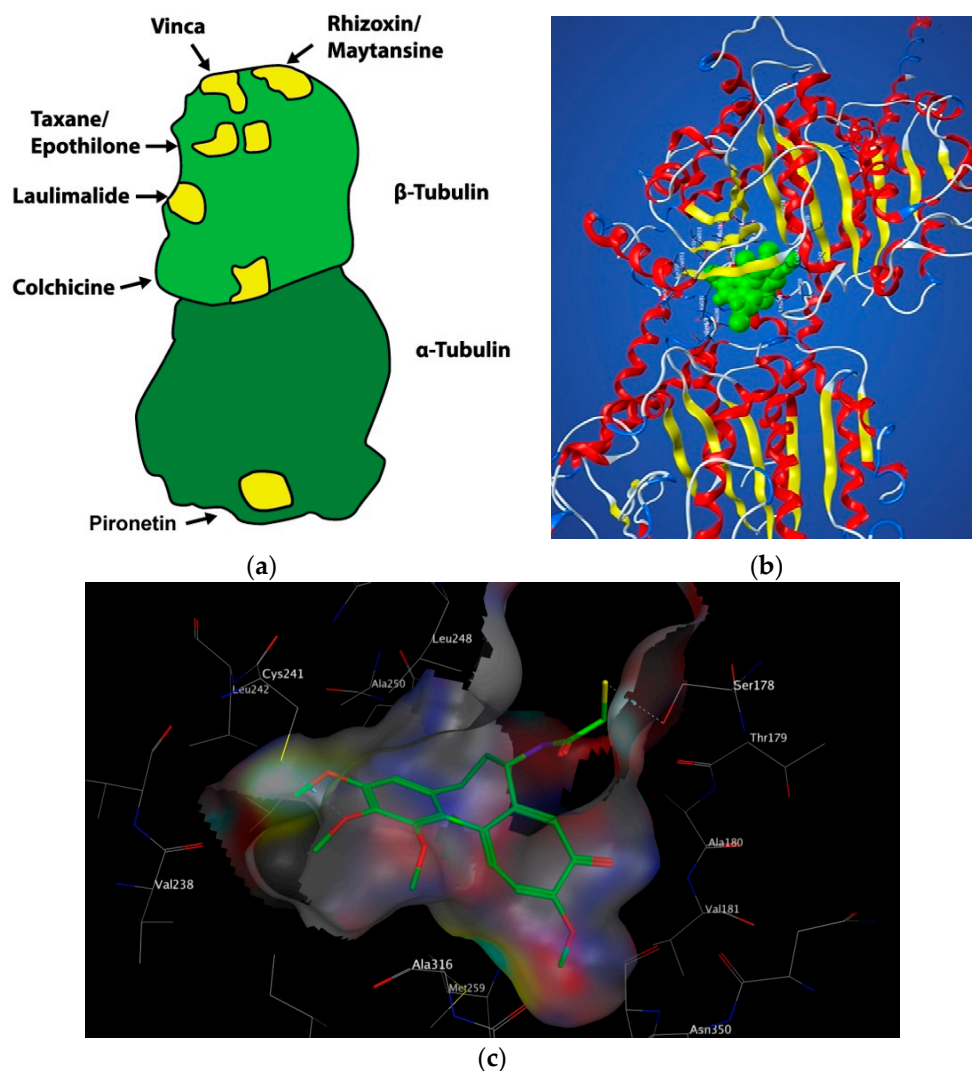


Figure 2. (a): Schematic representation of the different drug-binding sites on tubulin. (b): Space-filling model of colchicine (green) in the colchicine-binding site (CBS). (c): Model of N-deacetyl-N-(2-mercaptoacetyl) colchicine (DAMA)-colchicine bound at the interface of $\alpha\beta$ -tubulin. Key binding interactions are with Thr179 and Val181 of α -tubulin and Cys241 and Asn258 of β -tubulin. Colour key: green = carbon; red = oxygen; blue = nitrogen; yellow = sulphur.

2. Colchicine: Historical Uses, Structure and Mechanism of Action

Colchicine (1, Figure 3) is a tricyclic alkaloid (alkaloid nitrogen highlighted in blue, Figure 3) that is extracted from the plant *Colchicum autumnale*, also known as the autumn crocus or ‘poisonous meadow saffron’. Colchicine has been used as a medicine throughout history, with the first therapeutic use of *Colchicum autumnale* described almost 3000 years ago. It is a highly toxic anti-cancer MTA

and effectively inhibits cellular mitosis. Colchicine may also modify voltage-dependent anion channels of mitochondrial membranes, thereby limiting mitochondrial metabolism in cancer cells [8]. Therapeutic efficacy has been established for colchicine in the treatment of acute flares of gout and gouty arthritis [9,10]. It is also used to treat familial Mediterranean fever [11], Bechet's disease [12] and recurring pericarditis with effusion. Experimental medical use includes treatment of acute coronary syndromes [13]. This utilises colchicine's inhibition of a nucleotide-binding domain (NOD)-like receptor protein 3 (NLRP3) inflammasome protein complex, a novel pathway independent of colchicine's effects as an MTA. This suggests that colchicine has additional effects in addition to its potent antimetabolic potential [14,15]. Although a cheap chemotherapeutic option, colchicine's clinical applications are limited by its toxicity, narrow therapeutic index and the development of multi-drug resistance (MDR). Toxicity includes neutropenia, gastrointestinal upset, bone marrow damage and anaemia. Colchicine's toxicity is due to its antimetabolic properties. It binds to tubulin in non-cancerous cells and causes impaired protein assembly, mitotic arrest and multi-organ dysfunction [16].

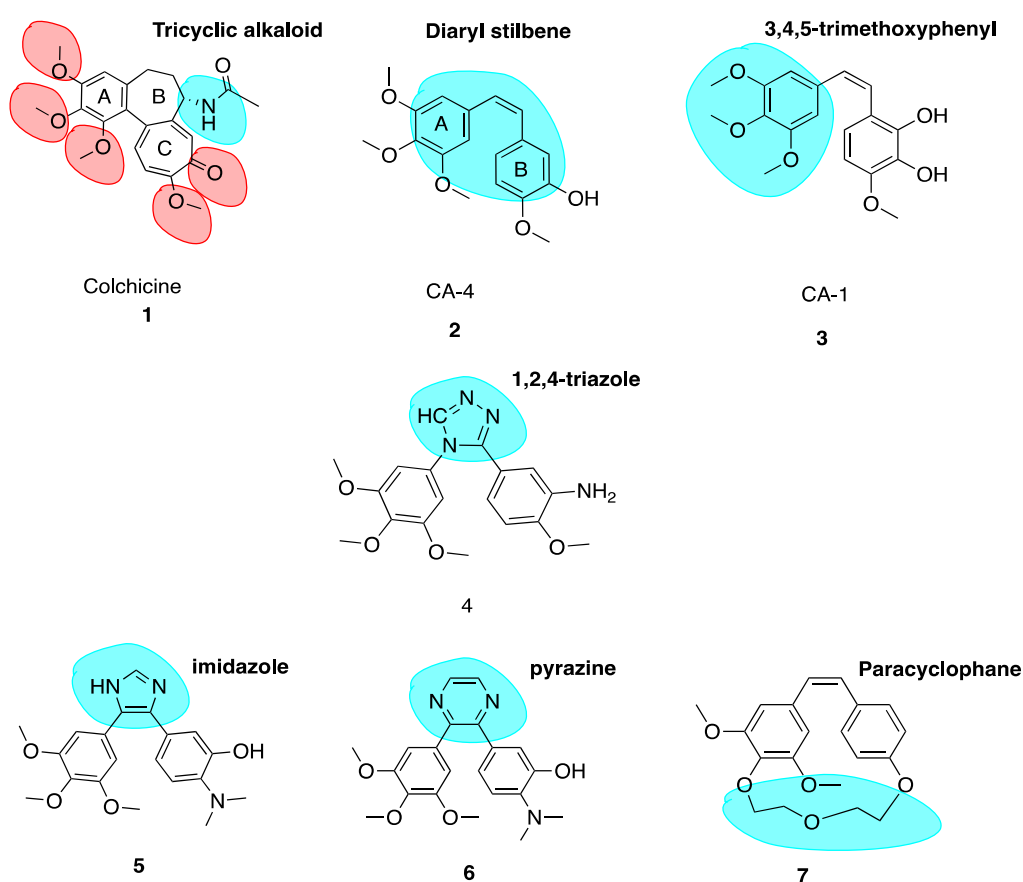


Figure 3. Structures of colchicine, combretastatin A-4, combretastatin A-1 and analogues 4–7.

Monomers of tubulin are divided into three functional domains: an amino terminal domain containing the GTP/GDP nucleotide binding region, an intermediate domain and a carboxy terminal domain [17]. Colchicine induces assembly independent GTPase activity to promote loss of the microtubule GTP cap and disassembly [18]. Upon colchicine binding to tubulin, the straight conformation of the $\alpha\beta$ -tubulin heterodimeric subunits is lost, resulting in curved tubulin heterodimers. Lateral contacts of adjacent $\alpha\beta$ -subunits necessary to maintain interactions between them are lost and, as lateral contacts decrease, microtubules disassemble. A steric clash between colchicine and α -tubulin inhibits microtubule assembly [19].

The CBS lies in the intermediate domain at the interface of α and β subunits (Figure 2). It was first characterised in 2004 by Ravelli et al. using X-ray crystallography. A 3.5 Å X-ray structure of $\alpha\beta$ -tubulin in complex with N-deacetyl-N-(2-mercaptoacetyl) colchicine (DAMA-colchicine) clearly outlined the structure of the binding pocket which has a width of 4–5 Å. The volume of the CBS site is mediated by helix 7 (H7) containing Cys β 241, loop 7 (T7) and helix 8 (H8). Experimental data demonstrates that colchicine binds to β -tubulin at its interface with α -tubulin, subsequently inhibiting tubulin polymerisation. The important trimethoxyphenyl group of colchicine is orientated within β -tubulin close to Cys β 241 [19].

Colchicine binds with high affinity to the β -subunit. It is surrounded by mainly β -tubulin through helix 7. Cys-241 hydrogen bonds with the trimethoxyphenyl ring of colchicine while Thr-179 and Val-181 within α -tubulin form hydrogen bonds with the tropolone ring [20]. There are stringent structural requirements for binding of colchicine to tubulin which have been extensively studied. Structurally the molecule consists of a 3,4,5-trimethoxyphenyl ring (the A ring), a saturated seven membered ring containing an acetamido group at position 7 (the B ring), and a tropolone ring (the C ring, 1, Figure 3). It has been shown that the strength of colchicine binding to tubulin is provided by the interaction of ring A with the CBS, whereas inhibition is modulated by interactions between the oxygen atoms on ring C and the CBS. It is proposed that ring A anchors and maintains the B and C rings in correct orientation within the binding locus. When the A ring structure is modified and anchoring is weakened, the free energy used to stabilise the complex in proper orientation may weaken its inhibitory effect on tubulin [18]. Changing the structure of colchicine's, a ring results in loss of binding affinity. B and C ring structural modifications are however possible [21].

The keto functional group on Ring C and the methoxy functional groups in Ring A and Ring C are crucial for binding of colchicine (highlighted in red, 1, Figure 3). Swapping the C ring keto and methoxy leads to inactive compounds. Ring C may be replaced with a regular benzene ring without loss of activity. Ring B's acetamido group is not essential for activity although the stereochemistry at this carbon is important likely due to the effect of this substituent on holding the molecule in overall conformation with respect to rings A and C [22].

3. Targeting the Colchicine-Binding Site for Anti-Cancer Therapy

Colchicine has been widely used as a research tool in the study of microtubules. Colchicine is known to stabilise microtubule structures at low concentrations and destabilise them at high concentrations bearing a similar mechanism of action to anti-cancer drugs, e.g., the vinca alkaloids. Drugs targeting the CBS have recently appeared on the market and it is anticipated that others will follow. There are several advantages of targeting the CBS, including the inhibition of angiogenesis and overcoming multidrug resistance (MDR).

Angiogenesis is one of the hallmarks of cancer. Angiogenesis plays a critical role in cancer as solid tumours require a blood supply with adequate oxygen and nutrients to grow beyond a few millimetres in size [23]. In recent years, emerging information on the environment of solid tumours has led to the consensus that there are several advantages of developing cancer therapies to target cancer cells indirectly by attacking the tumour vasculature [24,25]. Such compounds are called vascular disrupting agents (VDAs). VDAs target the tumour's established vasculature leading to haemorrhagic necrosis and subsequently cell death [26]. Microtubules are important regulators of endothelial cells and vasculature network formation and hence the CBS is an attractive target for VDAs. Colchicine's anti-vascular effects are often only observed at doses approaching or exceeding the maximum tolerated dose. Given the widespread clinical use of the taxanes and vinca alkaloids, research efforts are continuously focusing on developing colchicine-like VDAs as cancer treatments.

MDR is partially mediated by the overexpression of the ATP-dependent drug efflux pump, P-glycoprotein (P-gp). P-gp transports drugs out of cancer cells and away from their intended target. MDR is a major impediment to successful chemotherapy of human tumours. One of the major limitations of clinically used MTAs is the overexpression of the *MDR1* gene encoding for P-gp

in many tumour cells; it decreases intracellular drug levels and limits efficacy of cytotoxic agents. The overexpression of P-gp is correlated to poor response and treatment failure while using the taxanes and vinca alkaloids [27]. Additionally, the expression of a mutant β -tubulin III isoform is an indicator of resistance to paclitaxel and vinorelbine. CBSIs may remain unaffected by the expression pattern of β -tubulin [28]. The use of colchicine as an anti-cancer derivative is currently excluded based on its extreme toxicity, but this property does not exclude use of its scaffold as a template for generation of potent anti-cancer derivatives. Agents targeting the CBS are attractive as they are often effective in drug resistant models, as outlined throughout this review. They would provide another treatment option for cancer patients at a fraction of the cost of biologicals such as monoclonal antibodies.

4. Colchicine-Binding Site Inhibitors Known before 2017

4.1. Combretastatin A-4 and Analogues

The combretastatins are a group of diaryl stilbenoid (diaryl stilbene highlighted in blue, **2**, Figure 3) natural products which were isolated by Pettit et al. in 1989 from the bark of the South African bush willow tree *Combretum caffrum* [29]. *Combretum caffrum* belongs to Combretaceae family of shrubs found in South Africa, mainly of the Eastern Cape and Transkei to Natal. It was used for decades as a remedy for ailments ranging from heart and worm remedies, wound dressings and scorpion stings by the Xhosa tribe in South Africa [30]. Pettit et al. demonstrated that isolates from *Combretum caffrum* bark were active against murine lymphocytic leukaemia cell lines (P-388). This antiproliferative activity was later attributed to the combretastatin A series of compounds. In total, among 17 original natural combretastatins isolated, two *cis* stilbene compounds have attracted profound interest over the years. Combretastatin A-4 (CA-4, **2**, Figure 3) and combretastatin A-1 (CA-1, **3**, Figure 3) are the most potent analogues and have been the focus of much attention in areas of chemistry, biochemistry and clinical application. CA-1 may have enhanced potency relative to CA-4 due to its anti-vascular effects but also due to its potential to induce cancer cell death via an *ortho*-quinone mechanism, binding to cellular nucleophiles and forming free radicals [31].

The *cis* stilbene CA-4 has proven itself to be a significant cancer cell growth inhibitor and antimetabolic anti-cancer agent through the inhibition of tubulin polymerisation via binding at the CBS [32,33]. CA-4 is structurally related to colchicine, containing two phenyl rings tilted at 50–60° to each other, linked in *cis* geometry by a double bond and containing a 3,4,5-trimethoxyphenyl (highlighted in blue of CA-1, **3**, Figure 3) ring system. It binds in similar orientation as colchicine at the CBS. Both CA-4 and CA-1 and their respective phosphate prodrug salts, fosbretabulin (**83**, see the figure in Section 6.1.1) and Oxi4503 (**84**, see the figure in Section 6.1.1) are of increasing therapeutic interest. CA-4 shows promise in comparison to CA-1 in the potential treatment of tumours with acquired drug resistance [34].

CA-4 is not only considered to be an antimetabolic agent. In addition to its antiproliferative effects as an inhibitor of tubulin polymerisation, it also has potent anti-vascular and anti-angiogenic effects categorising it as a VDA. In 1997, Watts et al. noted an increase in endothelial permeability with CA-1. This indicated that the compound was targeting tumour vasculature and leading to cell death from ischaemic and tumour haemorrhagic necrosis. This selective disruption of tumour associated microvessels results in loss of nutrients, oxygen deprivation and ultimately necrosis [33]. The ability of typical MTAs namely vinblastine and colchicine to inhibit tumour growth via vascular mechanisms is well established [35]. Colchicine is not currently in clinical use as an anti-cancer treatment due to colchicine's narrow therapeutic index [36]. The phosphate derivative of CA-4P was found to inhibit tumour blood flow at concentrations 10-fold less than its maximum tolerated dose, which led to the first clinical trial of CA-4 as a VDA [37].

CA-4 appears to disrupt endothelial cell-specific junctional molecule vascular endothelial cadherin (VE-cadherin), which inhibits endothelial cell migration and capillary tube formation. The morphological changes induced on the endothelial cells lining micro vessels proceed to destroy the tumour from within [38]. CA-4 causes occlusion of the tumour vasculature, resulting in hypoxia-induced

necrosis, which targets the core of solid tumours [39]. This mechanism is unlike many other anti-vascular treatments which generally target peripheral but not core tumour cells, resulting in MDR. CA-4 appears to be specific for tumour endothelial cells, although the precise mechanism for selectivity over normal endothelial cells remains unclear. VDAs for cancer treatment are an attractive option as angiogenesis occurs in only a limited number of situations, for example, wound healing and during the menstrual cycle. Therefore, anti-angiogenic strategies hold potential for specificity with little toxicity.

CA-4's potential as an anti-cancer agent has long since been recognised, and it demonstrates potent cytotoxicity against MDR cancer cell lines [38,40]. Resistance to CA-4P monotherapy is seen however in the tumour rim [41]. This is likely due to additional support structures seen in mature vessels provided by the actin cytoskeleton, mature basement membranes and vessel-associated pericytes. This protects them from tubulin-binding disruption by VDAs. This suggests that combretastatin derivatives are ideal candidates to complement existing anti-cancer approaches, given that cells of the mature vasculature are more susceptible to conventional chemotherapy strategies [38]. Indeed, successes have been made in the clinical setting by combining combretastatin prodrugs with established therapy as will be discussed below in the section of this review on clinically used CBSIs.

4.2. Successful Modifications of Combretastatin A-4

CA-4 is a very potent anti-cancer agent. Its structural simplicity renders it amenable to chemical manipulation with the aim of modifying solubility, stability and therapeutic efficacy. CA-4 is typically observed to inhibit 50% of cancer proliferation within a dose range of 1–10 nM. It inhibits microtubule polymerisation in a dose range of 2–3 μ M. Many promising CA-4 analogues have analogous cytotoxicity and microtubule inhibitory properties. Thousands of analogues have been synthesised and described. CA-4 (2) is a fascinating lead molecule in design of CBSIs. This review aims to focus attention on recently emerging research on CA-4 derivatives with strong potential for further development as clinically used anti-cancer agents.

CA-4 can exist in two geometric configurations—*cis* and *trans* stilbene. The *cis* structure has been shown to be important for binding to the CBS. Only the *cis* configuration of CA-4 and other stilbene derivatives possess anti-cancer bioactivity. The active *cis* conformation of CA-4 readily isomerizes into the more thermodynamically stable but significantly less active *trans* isomer, demonstrating little or no biological activity [42]. Isomerization of *cis* CA-4 is readily observed on storage and additionally in vivo during metabolism accompanied by a dramatic reduction in both anti-tubulin and anti-tumour activity [43,44] recently reported due to structural distortion of *trans* CA-4 in the CBS [45].

CA-4 consists of three important structural features as briefly mentioned above. SAR studies have demonstrated that the following are crucial for tubulin polymerisation inhibitory effects:

- (1) 3,4,5-trimethoxyphenyl-substituted ring A.
- (2) 3-hydroxy-4-methoxyphenyl-substituted ring B.
- (3) *cis* double bond separating the two phenyl rings.

It is well known that the insertion of a heteroatom as a bioisostere in place of a carbon atom can yield new systems with modified pharmacodynamic and pharmacokinetic properties, including lipophilicity, polarity, aqueous solubility and importantly potency and selectivity [46]. A number of heterocyclic bridging CA-4 analogues have been prepared to restrict the *cis* configuration and provide optimal conformational geometry for interaction with the CBS. Oshumi et al. were the one of the first to replace the olfenic bond with a series of heteroatoms, prompted by observations upon superimposition of CA-4 and colchicine structures. A good match was seen, suggesting that the double bond region may in fact be amenable to expansion. A compound with a 1,2,4-triazole replacing the *cis* double bond (4, Figure 3) retained both cytotoxic and anti-tubulin activities, a significant advancement as the first successful replacement of the double bond by a ring structure with cytotoxic activity.

Synthesised combretastatin heterocycle derivatives to date include thiazoles, imidazoles, pyrroles, oxazoles, and many others [47]. Due to the increase in hydrophilicity of compounds containing lone pair

of electrons, upon the introduction of such heterocyclic moieties, these molecules have demonstrated improved water solubility with respect to CA-4 [48]. Many CA-4 analogues are highly potent tubulin inhibitors with nanomolar or picomolar antiproliferative IC_{50} values. However, certain *cis*-restrained analogues have reduced activity. Analysis of their structures can provide useful insight into why this may be the case. Three cases of structures that do not appear to be optimal for binding to the colchicine site of tubulin are:

- (1) Three-membered ring bridges,
- (2) Six-membered ring bridges, and
- (3) Immobilized trimethoxyphenyl moieties.

In an example of the first case, Fürst et al. replaced CA-4's double bond with a series of cyclopropyl units in an attempt to maintain the desirable *cis*-diaryl structural relationship. However, these compounds were significantly less active than corresponding stilbene derivatives. The cyclopropyl of CA-4 was found to have an IC_{50} of 0.028 μ M and 0.102 μ M in HeLa and MCF-7 cells respectively compared to 0.00051 μ M and 0.0025 μ M of CA-4. Despite low in vitro activity as an anti-cancer agent, cyclopropanes held less tendency to undergo *cis* to *trans* isomerization [49]. This illustrates that three membered ring bridges do not appear to be optimal for binding to the CBS. Secondly, replacing the double bond with a six-membered ring in all cases resulted in a large decrease in cytotoxicity. A good illustration is the replacement of an imidazole (5, Figure 3, highlighted in blue) ring with a pyrazine (6, Figure 3, highlighted in blue) ring resulted in a loss of 350 fold potency in non-small-cell lung carcinoma cell lines, with a dramatic increase in IC_{50} in NCI-H640 cells from 2 μ M (5) to 707 μ M (6) [50]. Thirdly, rigidifying the combretastatin trimethoxyphenyl moiety was an interesting possibility explored. Paracyclophane derivatives (e.g., 7, Figure 3) were synthesised, restricting the conformational freedom of the aryl rings with the polyether linkage with a polyether linkage between the A and B ring. These compounds did not possess any anti-angiogenic or biological activity [51]. These modifications provide important information on the structural tolerance of the CBS.

This review aims to highlight the most recent and exciting data for compounds with superior therapeutic efficacy to CA-4, discussing literature reports of structural modifications to CA-4 from 2017 to 2019 and selected others. Modifications of CA-4 have produced many synthetic derivatives with extremely potent antiproliferative and anti-tumour effects. A number of other reviews of CA-4 analogues have been published discussing prior modifications [3,52–55].

4.2.1. Potent Chalcone Derivatives of CA-4

Ducki et al. [56,57] used a chalcone scaffold to synthesise keto stilbene derivatives of CA-4 (8–12, Figure 4). They incorporated the aryl substitution pattern of CA-4 into their chalcones to obtain several compounds with potent in vitro antiproliferative activity at nanomolar concentrations against human chronic myelogenous leukaemia K562 cell lines, superseding the activity of CA-4. The introduction of an α -alkyl substituent to the enone improved potencies up to 20-fold. Compound 8 was roughly 200-fold less potent than 9, inhibiting cancer cell proliferation in K562 at an IC_{50} of 4.3 nM versus 0.21 nM for 9. The introduction of an alkoxy, e.g., SD400 (10, Figure 4), also increased the potency (IC_{50} = 1.5 nM). The α -methoxy chalcone 10 was identified as a potent inhibitor of tubulin assembly with an IC_{50} of 0.21 nM superior to CA-4's IC_{50} of 2.0 nM. K562 cells treated with these chalcones are blocked in mitosis consistent with classical CBSIs. The chalcones displaced colchicine from its binding site, confirming them as CBSIs. Compounds 8–12 have better activity in vivo than CA-4 in terms of vascular damaging properties. Conformational preferences for enone systems are generally *s-trans* unless forced into an *s-cis* arrangement by steric hindrance. Chalcone 8 adopts an *s-cis* conformation whereas the α -methyl chalcone 9 adopts the *s-trans*, suggesting that *s-trans* is good for bioactivity. The two aryl rings of chalcone 9 superimpose onto those of CA-4 better than that of 8 and therefore it is hypothesised that the introduction of the α -methyl results in stronger binding in the CBS. Despite

reports of pre-clinical studies for the phosphate prodrugs **11** and **12** (Figure 4), these compounds have not advanced into clinical studies [56].

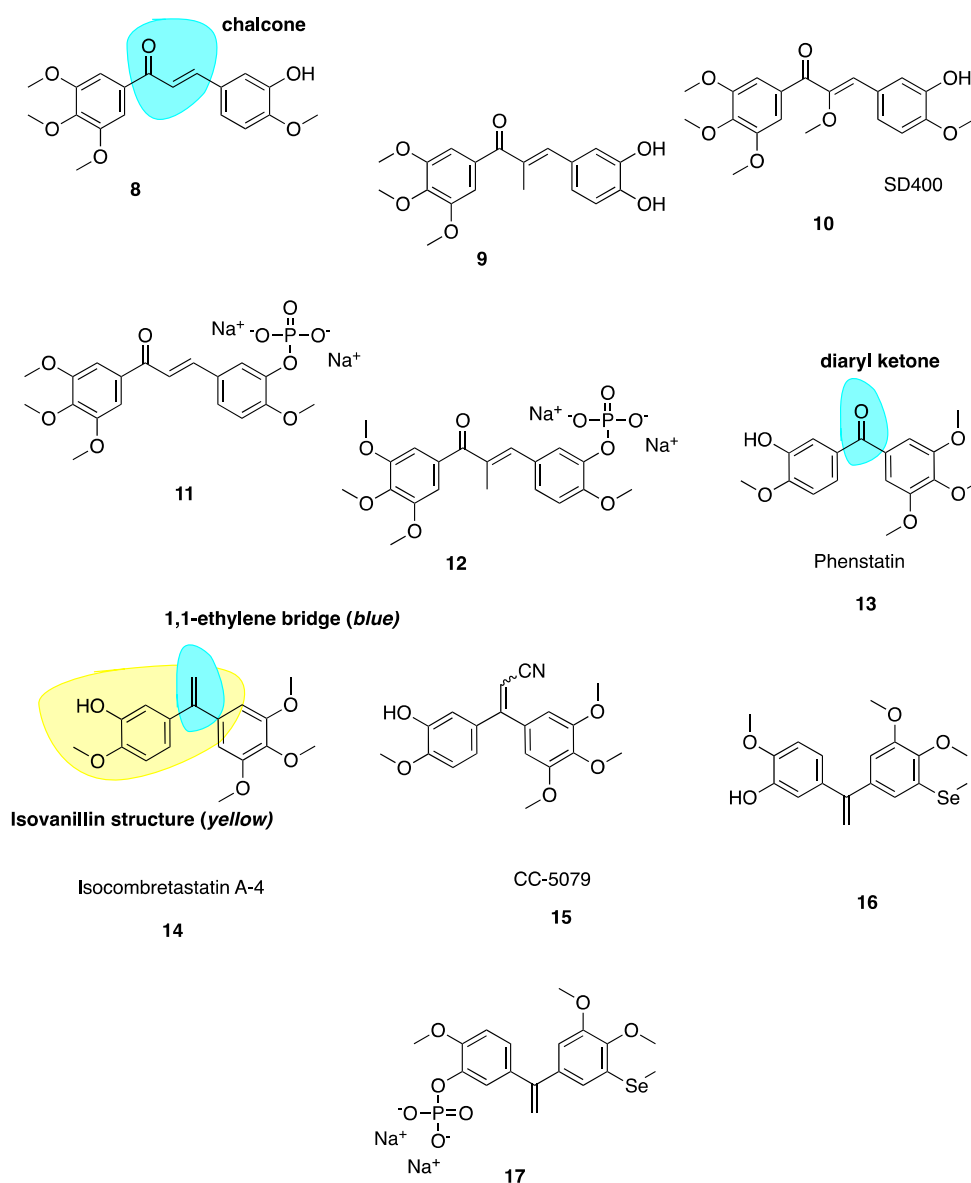


Figure 4. Combretastatin A-4 analogues 8–17.

4.2.2. Phenstatin and Derivatives

Diarylketone phenstatin (**13**, Figure 4) is a CA-4 analogue discovered serendipitously, where CA-4's olefin is replaced with a carbonyl group (highlighted in blue, Figure 4). It was obtained unexpectedly following Jacobsen oxidation; during an attempted epoxidation of CA-4 silyl ether to give the silyl ether of phenstatin. The deprotected benzophenone phenstatin is a potent cancer cell line growth inhibitor. This inhibitor is structurally related to the known CBSI, podophyllotoxin [58]. Phenstatin is more stable than CA-4 *in vivo* as it cannot isomerize to an inactive *trans* configuration [59]. It mirrors CA-4's biological mechanism of action and both phenstatin and its corresponding water-soluble prodrug salt demonstrate pronounced cytotoxicity against human cancer cell lines [60].

4.2.3. IsoCA-4 and Selenium CA-4 Derivatives

The 1,1-ethylene bridge (highlighted in blue, **14**, Figure 4) is regarded as a suitable bioisostere of the Z 1,2-ethylene bridge and has led to the development of potential *iso*CA-4 analogues. *Iso*CA-4 (**14**, Figure 4), with a 1,1-diarylethylene scaffold, is more active than phenstatin and colchicine ($IC_{50} = 2\text{--}5$ nM across a panel of cell lines) which are comparable values to CA-4 [61]. A diacrylonitrile derivative CC-5079 (**15**, Figure 4) had an IC_{50} of 3.0 nM comparable to 2.3 nM of CA-4 in HCT116 colorectal cancer cells [61]. During a screening program, it was found that **15** had potent antiproliferative and anti-tubulin effects on human umbilical vein endothelial cells (HUVECs) as an inhibitor of tubulin polymerisation, was associated with G2/M phase arrest and was active against MDR cell lines. It significantly inhibited growth of *in vivo* xenograft colorectal mouse tumour models [62]. Further to this work it was found that **15** inhibited angiogenesis *in vitro* and *in vivo*, potently inhibiting microvessel formation [63]. No further clinical development has occurred with these compounds.

Few selenium containing CA-4 analogues are known in the literature. Those studied include selenium atoms as spacer groups between CA-4's A and B aryl rings. Antiproliferative successes are good with similar anti-cancer potencies to CA-4 [64–67]. Pang et al. have prepared a series of organoselenium compounds obtained by introducing a methyl(phenyl) selene to *iso*CA-4 and phenstatin. Most of these compounds exhibit excellent and potent antiproliferative activity against human cancer cell lines. The most successful compound **16** (Figure 4) demonstrated low nanomolar potency with IC_{50} values of 3.9 nM in A549 cells, 2.2 nM in MDA-MB-231 cells and 3 nM in HEPG2 cell lines. Compound **16** also exerted successful antiproliferative activity against cisplatin resistant cell line A549/CDDP and doxorubicin resistant cell line HEPG2/DOX. The phosphate salt **17** (Figure 4) was tested against A549 xenograft tumours, resulting in an inhibitory rate of 72.9% compared to 47.6% of CA-4P and 52.2% of *iso*CA-4P, without apparent toxicity. Mechanistic studies demonstrate that the introduction of the selenium atom to *iso*CA-4 elevated its anti-cancer properties while retaining tubulin polymerisation inhibition, cell cycle arrest and apoptosis induction [68].

4.3. New Combretastatin A-4 Analogues Reported between 2017 and 2019

4.3.1. New Combretastatin A-4 Analogues of 2017

β -Lactam *Cis* Restricted Analogues

Our group has extensively reported a series of antiproliferative, tubulin-binding β -lactam compounds—the 'combretazets', which have greater tubulin depolymerization potency with respect to CA-4 [69]. Prior to our research, it was known that β -lactam-containing compounds possessed antiproliferative activity [70,71]. The introduction of the rigid β -lactam bridge (highlighted in blue, **18**, Figure 5) scaffold allows similar structural arrangement between CA-4's two aromatic rings, overcoming double bond *cis/trans* isomerization by substituting the ethylene bridge for a 1,4-diaryl-2-azetidinone ring [69,72–74]. The rigid ring scaffold permits the similar spatial arrangement between the two aromatic rings as observed in non-planar *cis* conformations of CA-4.

These β -lactam bridge analogues of CA-4 have demonstrated significant tubulin depolymerising effects in human breast cancer cell lines [69,72–75]. Malebari et al. expanded the previous work of Greene et al. [69] on compounds **18** and **19** (Figure 5), which had IC_{50} values of 38 and 19 nM respectively in MCF-7 cells. Compounds with B ring *meta*-hydroxyl substituents, such as **18**, were far less active in combretastatin refractory HT-29 (human colorectal adenocarcinoma colon cancer) cells [76]. Substitution or deletion of the B ring *meta*-hydroxyl group at the 4-position of the β -lactam ring to produce compounds such as **20** (Figure 5) led to potent activity in HT-29 cells. **20** had an IC_{50} value of 12 nM in HT-29 cells, contrasting with CA-4's micromolar IC_{50} of 4.17 μ M. Formation of a glucuronide metabolite is the main metabolic pathway by which CA-4 is cleared [77] and it is likely that glucuronidation is a method of intrinsic drug resistance in adenocarcinoma cells such as HT-29 cells [78].

Deletion of the B ring hydroxyl group slows glucuronidation by uridine 5-diphosphoglucuronosyl transferase enzymes (UGTs) in HT-29 cells and contributes to the potent activity of these β -lactams.

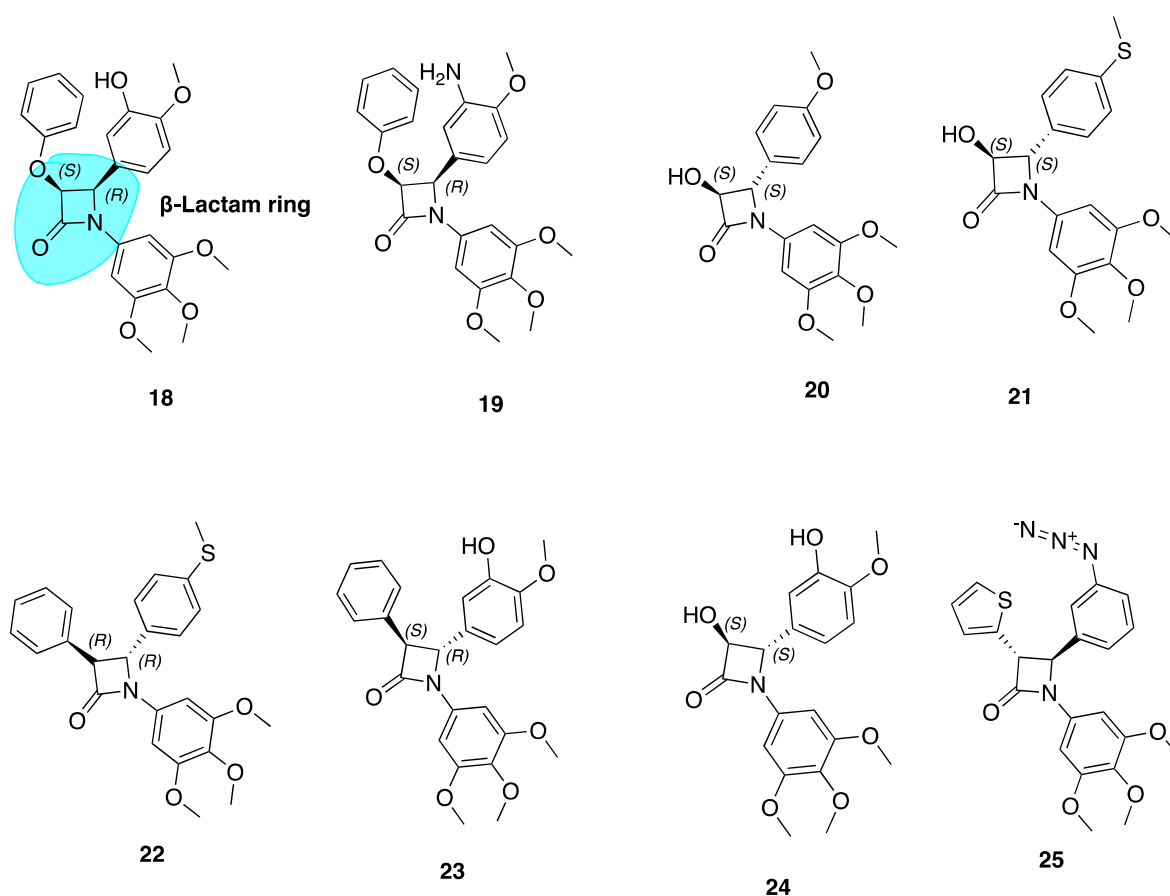


Figure 5. Structures of β -Lactams 18–25. (*Cis* isomers of 18 and 19 and *trans* isomers of 20–24 isolated only. (One enantiomer represented for each compound).

Analogues with thioether moieties in Ring B such as 21 and 22 (Figure 5) had potent antiproliferative activity in three cancer cell lines—MCF-7, HL-60 and HT-29. Interestingly the thioether β -lactams demonstrated excellent effects in HT-29 cells (IC_{50} values of 15 and 56 nM respectively). This demonstrates the ability of a thioether substituent to slow or avoid UGT-induced metabolism in this series of compounds, positioning them as lead compounds for resistant colon cancers. These compounds disrupt microtubule structure in both MCF-7 and HT-29 cells by inducing G_2/M phase arrest and apoptosis [76]. Hence, CA-4's B ring may provide fertile grounds for activity optimization of novel analogues for the treatment of MDR colon cancers. These compounds show promise for further clinical development having introduced two major modifications to prevent inactivation; firstly via isomerisation (*cis* restriction by replacement of the double bond with a β -lactam ring) and secondly via metabolism by glucuronidation (deletion of B ring *meta* hydroxyl group).

Compounds 22–24 showed extremely high nanomolar potency in MCF-7 and HL-60 cell lines. IC_{50} values for 22, 23, and 24 in MCF-7 cells were 4 nM, 4 nM, and 3 nM respectively. This emphasises the importance of the *meta*-hydroxyl for optimum activity in breast cancer cells, a large contrast to the Ring B's detrimental role in terms of anti-cancer activity towards colon cancers.

β -Lactam CA-4 Analogues with an Azide Substituted B Ring

β -Lactam 25 (Figure 5) was the most active of a series of azide derivatives synthesized by Fu and co-workers as an orally active CA-4 azide derivative. It acts as a tubulin polymerization inhibitor and

antimitotic agent with similar biological effects to the aforementioned β -lactam derivatives (G_2/M phase cell cycle arrest and apoptosis). Fu et al. describe replacing a phenyl at the C3 β -lactam ring position with a thiofuran sulphur-containing moiety to increase antiproliferative potency. The position of the azide is important for antiproliferative potency. Moving the N_3 from *para* to *meta* position, as in **25**, greatly improved potency with IC_{50} values ranging from 0.106–0.507 μM compared to values of 0.154–4.203 μM in MGC-803, MCF-7 and A549 cells. Replacement of the azide structure with bulky groups such as 1,2,3-triazoles and long carbon chains had detrimental effects on antiproliferative potency. This demonstrated the importance of small substituent groups on CA-4's B ring as large groups appear unfavourable for antiproliferative efficacy. In a xenograft model of MGC-803 tumour cells, **25** caused significant suppression of tumour growth without apparent toxicity and with comparative efficacy to CA-4P. This data suggests that **25** may serve as a new candidate for further investigation [79].

4.3.2. New Combretastatin A-4 Analogues of 2018

Dihydronaphthalene Derivatives

Maguire and co-workers utilized the dihydronaphthalene molecular scaffold (highlighted in blue, Figure 6) to synthesise two CA-4 derivatives KGP03 (**26**, Figure 6) and KG413 (**27**, Figure 6) as promising inhibitors of tubulin polymerisation. Their work was based on prior investigation of Oxi8006 (**28**, Figure 6), an indole derivative [80] and phenstatin (13) [58,81]. Compounds **26** and **27** were found to have IC_{50} values for the inhibition of tubulin polymerisation of 0.46 and 0.85 μM , akin to CA-4 ($IC_{50} = 1.2 \mu M$). This prompted evaluation of corresponding water-soluble prodrugs KGP04 (**29**) and KGP152 (**30**, Figure 6) in in vivo models of human cancers using murine models of MDA-MD-231 breast orthotopic tumours utilising bioluminescence imaging (BLI). Further, **30** induced vascular shutdown at 4 h, with a decrease of 99% relative to control in light emission, which had only recovered to 81% by 24 h after administration. Similarly, KGPO4 (**29**) was administered in a rat model of human lung cancer with a human A549 tumour xenograft. Vascular shutdown as measured using Doppler Colour ultrasound was seen as early as 2 h following administration. The dihydronaphthalene analogues appear to be promising candidates for further development as VDAs [82].

Quinazolinone Derivatives

Wolfgang et al. have investigated 3,4-dihydroquinazolin-2(1H)-one (highlighted in blue, Figure 6) derivatives as CBSIs. Through replacement of steroidal motifs of 2-methoxyestradiol, while maintaining essential pharmacophore regions, they synthesized a derivative with nanomolar potency (**31**, Figure 6) (GI_{50} of 50 nM in DU-145 and MDA-MB-231 cells). Tetrahydroisolquinoline moieties were used to mimic A and B steroidal rings, while the N-2 position is tethered to a benzyl group mimicking the steroidal D ring. This series sees the introduction of methoxyl benzyls at this N-2 position with the aim of producing a steric clash between the benzyl ring and N-2 position. A steric clash places a H-bond acceptor group near an optimal binding target at the CBS. Indeed, co-crystallization of **31** with the $\alpha\beta$ -tubulin heterodimer demonstrates that **31** binds more deeply than colchicine itself. The sulfamate group is shown to be a mediator of this affinity with β -tubulin, the first example of a sulfamate ester bound to tubulin. Future studies will potentially involve evaluation of this compound in animal models [83].

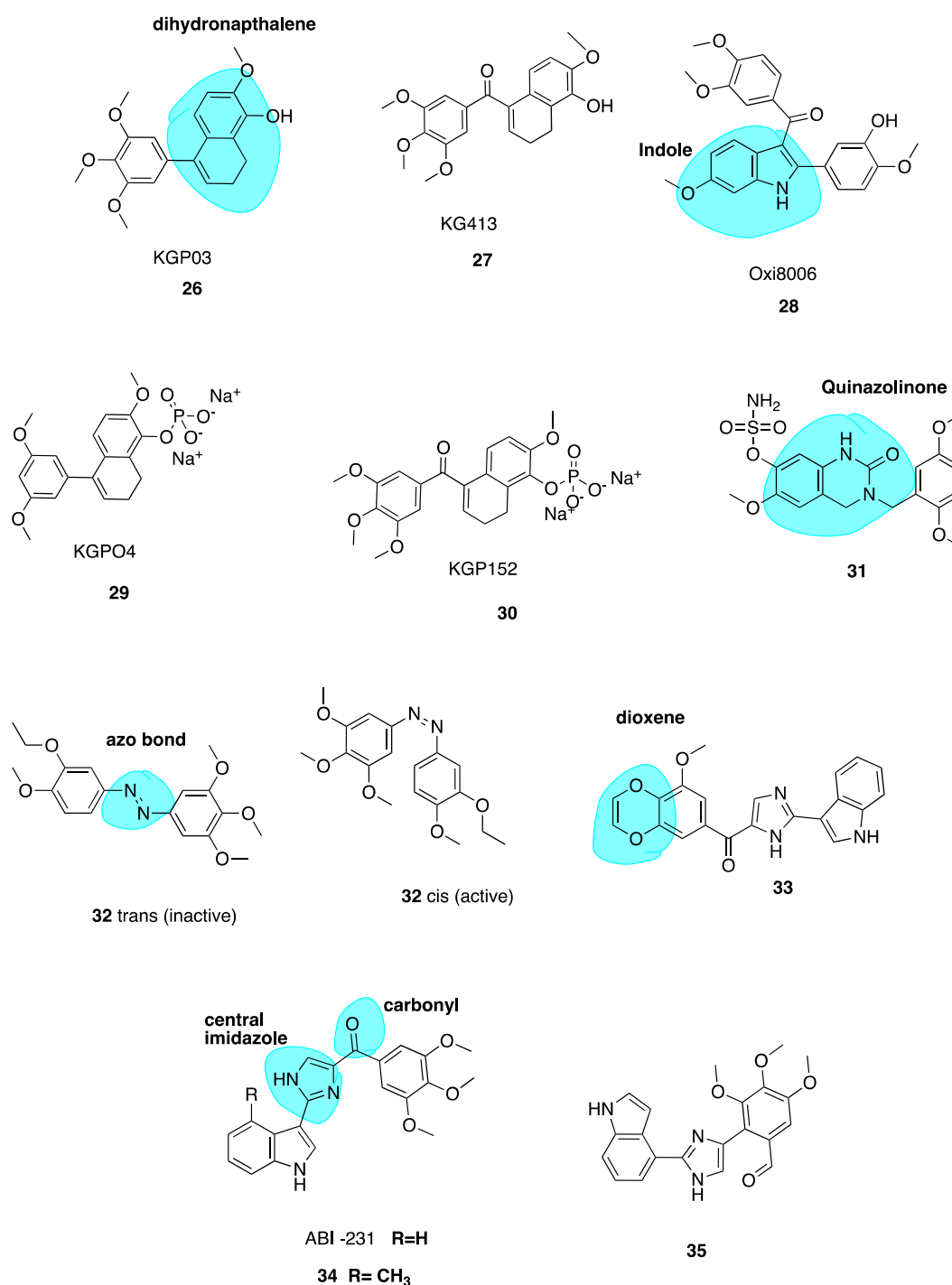


Figure 6. Structures of compounds 26–35.

Photo-Responsive Azo CA-4 Analogues

Rastogi et al. [84] have adopted an interesting approach to improve the potency and stability of CA-4 as a cytotoxic agent, recognising the promise of a photo-responsive approach in the area of MTAs. They note that while non-isomerizable analogues of CA-4 may display more potent anti-cancer activity, there still remains issues with drug specificity. This problem persists as the molecules are non-selective towards normal and cancer cells. To address this issue of tissue selectivity they have designed a series of potent photo-responsive analogues of CA-4 in which the double bond is replaced by an azobenzene structure (highlighted in blue, Figure 6). This has previously been investigated by

two other groups [85,86]. Using UV light in ranges of 395–400 nm, it is possible to convert an inactive *trans* isomer to *cis* bioactive derivatives in a selective manner. Photo-pharmacology is a potentially powerful tool to selectively target chemotherapy towards cancer cells only. Biological functions can be controlled by applying light to localized areas, achieving in vivo accuracy to overcome poor specificity in drug delivery [87–89].

The focus of the work of Rastogi et al. was to modify the B ring in order to improve potency of these analogues. *Trans* compound **32** (Figure 6) had IC₅₀ values of 60 and 110 µM in HeLa and H157 cells in the dark respectively. Upon irradiation to the *cis* compound **33** using 390–400 nm wavelengths of UV light, the antiproliferative activity improved 550-fold. This technique shows promise for site specific activation of chemotherapy, a very interesting and emerging approach. The photoresponsiveness of these analogues is easily seen using UV-spectroscopy, monitored by $n-\pi^*$ and $\pi-\pi^*$ transitions [82].

Replacement of the Trimethoxyphenyl Moiety

Wang et al. recently investigated the replacement of the essential 3,4,5-trimethoxy moiety of CA-4 for improvement of antiproliferative and tubulin binding activity. Modifying this portion of CBSIs is typically unsuccessful in improving antiproliferative potency. Crystallography work of analogues by this group demonstrated that only one methoxy moiety was involved in an interaction with Cys-241 of β -tubulin. Hence, the other two methoxys could be modified to improve antiproliferative activity. This resulted in **33** (Figure 6), the most potent of the series, containing a unique 3-methoxybenzo-[4,5]-dioxene moiety (highlighted in blue, Figure 6). It demonstrates IC₅₀ values ranging from 1.1–3.3 nM in several melanoma cell lines. Co-crystallisation with tubulin has confirmed its direct binding to the CBS, demonstrating that the A ring of CA-4 may indeed be further optimized to improve potency [90].

4.3.3. New Combretastatin A-4 Analogues of 2019

ABI-231 Analogues

Chen et al. have recently reported novel analogues of ABI-231 (Figure 6), one of their most potent orally bioavailable CBSIs with a bicyclic heterocycle pharmacophore, central imidazole and carbonyl linker (highlighted in blue, Figure 6) [91,92]. Amongst all of this group's scaffolds, ABI-231 is by far the most potent and successful antiproliferative compound having an average IC₅₀ of 5.2 nM in terms of antiproliferative activity across a large panel of cell lines. Additionally, ABI-231 inhibits the expression of mutant tubulin isotypes inclusive of β III and β IV tubulin thus restoring cellular susceptibility towards the action of typical MTAs, supporting its use to surmount MDR [93]. The authors have extensively investigated SAR of the 3-indole moiety to provide a rationale for molecular interactions at the CBS. They identified two superior analogues **34** and **35** (Figure 6). X-ray crystallography confirms unique and direct binding to the CBS demonstrating superior interactions to β -tubulin to explain increased antiproliferative activity. Both analogues successfully disrupt tubulin polymerisation, promote microtubule fragmentation and inhibit cancer cell migration. Compound **34**, the 4-methyl analogue of ABI-231, demonstrated the best inhibitory effects with an IC₅₀ range from 1.7 to 3.2 nM in A375, MI4 and WMI64 cells which is 3-fold more potent than parent ABI-231. Compound **35** was synthesised based on the hypothesis that an indolyl rotation may increase binding affinity at the CBS and augment antiproliferative activity [94]. The 4-indolyl analogue showed approximately two-fold improvement in activity compared to ABI-231 with IC₅₀ values ranging from 1.6–3.7 nM in the aforementioned cell lines compared to 5.6–8.1 nM for parent compound ABI-231. These compounds are active against MDR cell lines, including those resistant to paclitaxel, thus circumventing P-gp-mediated resistance. Compound **35** demonstrated high potency in the inhibition of tumour growth in a prostate paclitaxel resistant mouse xenograft model, suggesting that it may be a promising compound for certain MDR cancer types [95].

3-Vinyl Substituted β -Lactams

Our group reported a series of 3-vinyl β -lactams with potent anti-tubulin and antiproliferative effects on breast cancer cells. Compound **36** (Figure 7) was the most potent of the series with a mean GI_{50} value of 23 nM when tested across the National Cancer Institute panel of cell lines. In particular, this compound showed potent activity in the MCF-7 breast cancer cell line with an IC_{50} of 8 nM, comparable to CA-4. Compound **36** inhibited tubulin polymerisation 8.7-fold at a concentration of 10 μ M. This study demonstrated that a hydrophobic substituent at C-3 of the β -lactam ring may enhance biological activity. Preliminary docking studies revealed that the vinyl substituent sits in the CBS. These results are promising for further development of the β -lactam structures as more stable analogues of CA-4 [72].

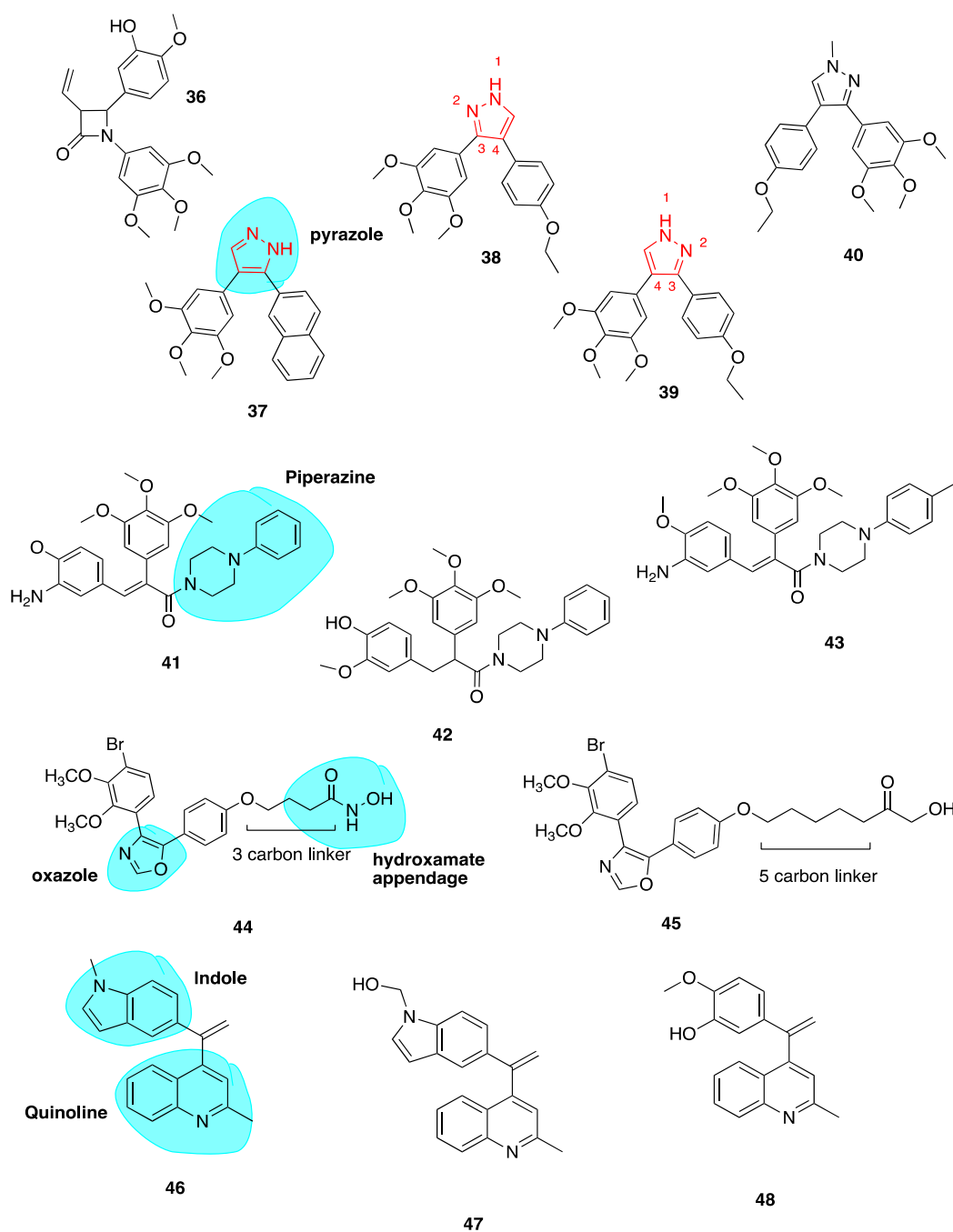


Figure 7. Structures of combretastatin analogues **36–48**.

Pyrazole Analogues

Romagnoli et al. previously published a series of potent analogues in which CA-4's ethylene bridge is incorporated into 3,4-diaryl substituted 1*H*-pyrazoles (highlighted in blue, Figure 7) and tetrazoles [96, 97]. This work was based on the work of Medarde and co-workers from 2005, who described 3,4-disubstituted pyrazole derivatives of CA-4. Their most potent inhibitor of tubulin polymerisation, compound 37 (Figure 7), had an IC₅₀ value of 33 µM compared to 3 µM of CA-4 [98].

Despite CA-4's potency in many cancer cell lines, it is ineffective against HT-29 colon cancer cells. Two analogues 38 and 39 (Figure 7) with a 4-ethoxyphenyl at either the C-4 position (38) or C-3 position (39) of the 1*H*-pyrazole ring show great promise in these cell lines. While previous work involving the use of a pyrazole *cis* restricted CA-4 analogue resulted in compound 37 demonstrating potencies of 3.3–28.4 nM across a range of cancer cell lines, by comparison 39 demonstrated superior in vitro inhibitory effects on tumour cell proliferation across all cell lines with superior IC₅₀ values of 0.06–0.7 nM. Interestingly 39 was most effective in HT-29 cells, a cell line with known resistance to CA-4 due to the expression of UGTs. As mentioned above, the overexpression of UGTs leads to glucuronidation of CA-4's *meta* hydroxyl group of Ring B [76].

As 38 also demonstrated subnanomolar IC₅₀ values, it was concluded that the position of 3,4,5-trimethoxyphenyl at C-3 or C-4 of the 1*H*-pyrazole had little effect on the antiproliferative activity. On the contrary, the position of the aromatic rings at the 3 or 4 position of the 1*H*-pyrazole system affected the potency with 39 being 4–6 times more potent than its isomeric counterpart 38 with the exception of HeLa cells. Both 38 and 39 successfully inhibited tubulin polymerisation, indicating that a pyrazole can substitute successfully for CA-4's double bond. Both compounds show cytotoxicity against CEM^{Vbl-100} cell line which is an MDR cell line overexpressing the P-gp efflux transporter [99]. This indicates that these derivatives are not substrates of P-gp. Compound 39 also prevented cell migration in an MDA-MD-231 breast cancer cell model. Compounds 38 and 39 were evaluated for cytotoxic potential in peripheral blood flow lymphocytes in healthy donor cells and non-cancerous human astrocytes. Both compounds had IC₅₀ values greater than 10 µM, together suggesting low toxicity in normal cells in comparison to tumour cells. This preliminary data is particularly promising as neurotoxicity is a major limiting factor in the clinical use of antimitotic agents. Lead compound 39 was assessed in a mouse allograft tumour model using E0771 murine breast cancer cells and preliminary results show reduction in tumour burden comparable to CA-4P, with no toxic effects or weight loss [97].

A series of pyrazole *cis*-restricted CBSIs was also recently described, including novel analogue 40 (Figure 7) which introduces a methyl at the N-1 position of the pyrazole ring. Compound 40 is an analogue from a series of 1,4-substituted-3-(3,4,5-trimethoxyphenyl)-5-aminopyrazole analogues of CA-4. 40 had the best antiproliferative activity with an IC₅₀ comparable to CA-4 of 17 nM and 31 nM in ovarian cancer cells and triple-negative breast cancer cells respectively. Larger bulky groups replacing the N-1 methyl were not tolerated. Crucial SAR contributions were the 4-ethoxy and 4-methylthiol on the B ring, with 3-methoxy groups reducing activity. This group demonstrated that by placing the A ring at the C4 position instead of the C3 position, only a minor effect in activity was observed. Pyrazole 40 was administered to mice containing 200 cm³ human ovarian adenocarcinoma xenograft model tumour. It resulted in reduction of tumour growth compared to vehicle by 62.8% whilst being well tolerated. Compound 40 exhibits typical cellular effects of CBSIs, including G₂/M phase arrest, apoptosis, the inhibition of cancer cell migration and disordered spindle formation/microtubule polymerization [100].

Piperazine Conjugates

Our group has recently described a series of CBSIs which consists of piperazine-substituted derivatives (highlighted in blue, Figure 7) of CA-4 formed via two-step Perkin microwave synthesis and amine conjugation. Piperazine may improve water solubility of drug molecules due to the presence of a heteroatom and in this case was chosen to prevent unwanted *cis* to *trans* isomerisation of CA-4. Three compounds 41, 42 and 43 (Figure 7) had submicromolar IC₅₀ values in MCF-7 cells during

preliminary in vitro screening. Docking studies indicate that the trimethoxy A rings overlay with those of DAMA-colchicine, whilst the B ring of the piperazine conjugates align with the C ring of DAMA-colchicine. Toxicity of the compounds is minimal and water-soluble conjugates will be developed for the potential treatment of triple-negative breast cancer [101].

Oxazole-Bridged Analogues

Schmitt et al. published a series of novel pleiotropic CA-4 derivatives which includes both CBSIs and inhibitors of histone deacetylase enzymes (HDACs). It is known that HDACs are overexpressed in various solid tumours [102]. Sole HDAC inhibitors have shown shortcomings in treatment of solid tumours. In order to overcome such drawbacks, inhibitors termed designed multiple ligands with dual or multimodal actions are sought after [103]. HDAC inhibitors show synergistic effects in combination with tubulin-binding anti-cancer drugs. This group describe a series of tubulin-targeting oxazole-bridged derivatives with hydroxamate appendages (highlighted in blue, **44**, Figure 7) [104]. These compounds were potent antiproliferative compounds against Ea.Hy926 cells (endothelial hybrid cells) with IC_{50} values ranging from 1.2 to 410 nM, with selectivity over non-malignant human dermal fibroblasts (HDFa cells; IC_{50} 23.9 to >100 μ M). Antiproliferative activity was strongest with decreasing linker length. Compound **44** (Figure 7) containing a 3-carbon linker completely inhibited tubulin polymerization at a concentration of 10 μ M. In contrast, compound **45** (Figure 7) containing a 5-carbon linker, showed no inhibition whatsoever, supporting the theory that cytotoxic effects of the compounds decrease with increasing carbon chain length via absence of tubulin inhibition. Compound **45** in contrast was the most potent HDAC6 inhibitor demonstrating the need to find a balance between the two activities. Compound **44** is a promising drug candidate with antiproliferative, cell cycle arresting, microtubule-destabilizing effects in addition to HDAC inhibition. In vivo investigations are underway [104].

Quinoline and Indole Derivatives of *iso*CA-4

Li et al. synthesised **46** and **47** (Figure 7), where CA-4's 3,4,5-trimethoxyphenyl and *iso*CA-4's isovanillin moieties are replaced with a quinoline moiety and indole moiety respectively (highlighted in blue, **46**, Figure 7). The use of the quinoline moiety is based on work by Khelifi et al. in which a quinoline structure was predicted by docking studies to form a hydrogen bond with Cys-241 residue of the CBS through the *N*-1 atom of the quinoline ring. Quinoline **48** (Figure 7) displayed nano- and sub-nanomolar levels of cytotoxicity against five cancer cell lines and inhibited tubulin polymerization with micromolar IC_{50} values [105].

The adoption of the indole moiety in place of the isovanillin structure resulted from studies demonstrating its occurrence in CBSI's as a replacement for *iso*CA-4's isovanillin ring moiety [106–108]. Compounds **46** and **47** showed most potent activity against leukemic K562 cells and five other cancer cell lines with IC_{50} values ranging from 5 to 11 nM, comparable to those of CA-4. In vivo anti-tumour activity was evaluated for both leads in a liver cancer xenograft mouse model. Interestingly **46** and **47** reduced tumour weight by 63.7% and 57.3% respectively without apparent toxicity. Both compounds were more potent than CA-4 which inhibited tumour growth by 51%. Collectively these results highlight the potential in further development of **46** and **47** as tubulin-targeting anti-cancer drugs [109].

Heterocyclic *iso*CA-4 Derivatives

Naret et al. have undertaken the challenge of optimizing *iso*CA-4 analogues with heterocycles replacing both traditional A and B rings, where the 3,4,5-trimethoxyphenyl A ring is replaced by a pyrimidine-dionyl, quinolinylyl or a quinazolinylyl while the B ring is substituted by a carbazolyl or indolyl group. Compound **49** (Figure 8) resulted with highest potency with a quinaldine moiety as ring A and an *N*-methylcarbazole (highlighted in blue, Figure 8) in place of ring B. Compound **49** was more active than *iso*CA-4 against A549, U87-MG and HUVEC cells and it was 67-fold more potent than CA-4 in lung adenocarcinoma epithelial cells (A549). When tested in a range of MDR cells lines, **49** was

up to 27 times better than *iso*CA-4 and CA-4, including against HT-29 cells (IC₅₀ of 3 nM compared to 265 μM and >8000 μM for *iso*CA-4 and CA-4 respectively) [110]. It has a high logP value of 5.26 and therefore potentially could partition through the blood-brain barrier. Combined with activity against human glioblastoma cell lines (U87-MG, IC₅₀ = 1.9nM), 49 could potentially serve as a candidate for the treatment of glioblastoma, an exciting prospect for the novel compound [108].

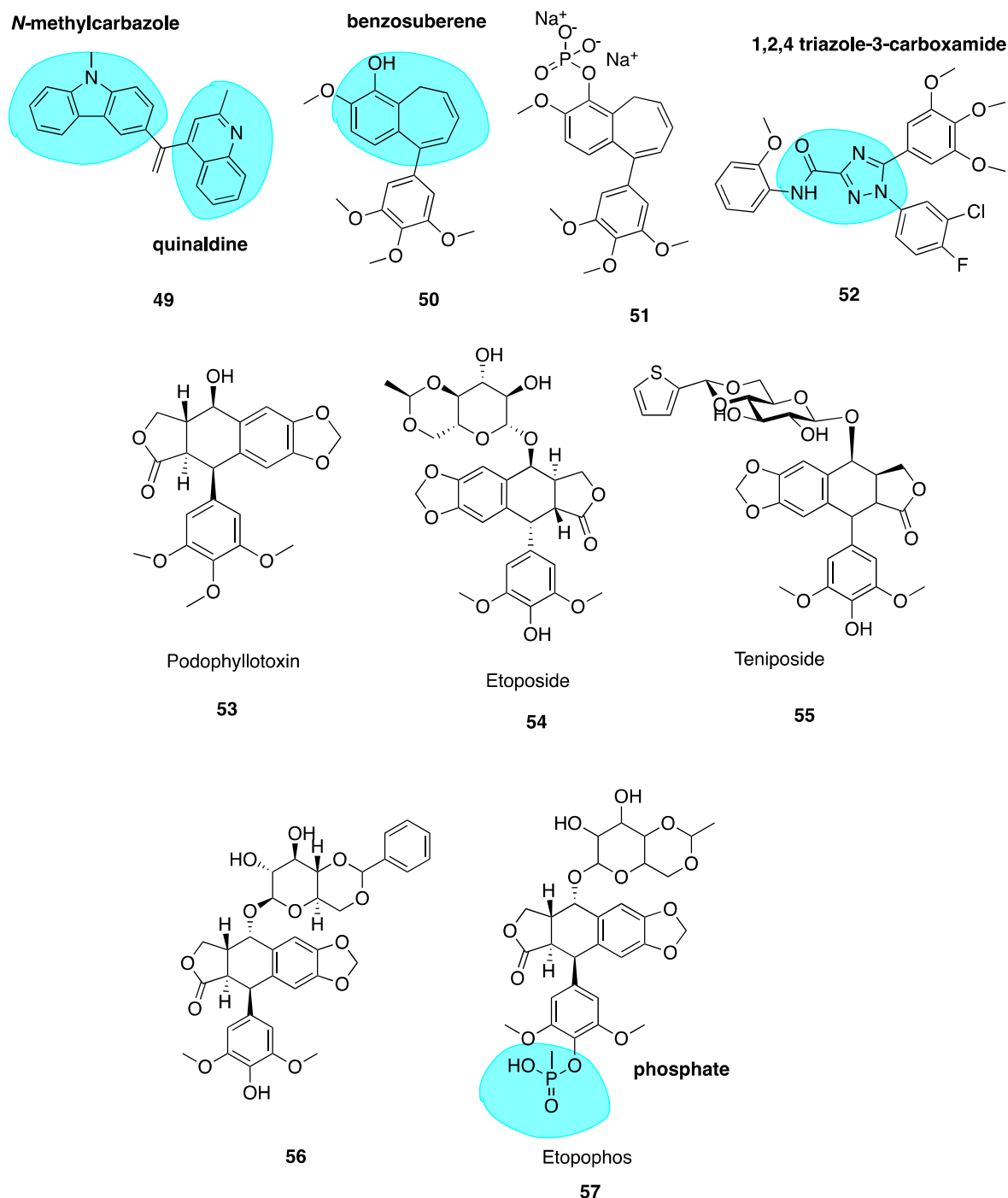


Figure 8. Structures of heterocyclic *iso*CA-4 derivative 49, novel benzosuberene analogues 50 and 51, carboxamide derivative 52, podophyllotoxin 53, etoposide 54 and analogues 55–57.

Novel Benzosuberene Analogues

Niu et al. replaced the double bond of CA-4 with a benzosuberene (highlighted in blue, Figure 8) ring structure to yield compounds **50** and **51** (Figure 8), with an IC₅₀ of 6.9 nM in the ovarian cancer cell line SK-OV-3. The phosphate prodrug **51** showed dose-dependent vascular shutdown comparable to CA-4 [111].

1,2,4-Triazole-3-Carboxamide Derivatives

A new study has recently been published using a 1,2,4-triazole-3-carboxamide scaffold (highlighted in blue, Figure 8) to replace the stilbene double bond of CA-4. Compound **52** (Figure 8) was the most potent analogue of the synthesized series, with an IC₅₀ of 4 nM in HL-60 cells, an excellent example of the introduction of fluorine leading to enhanced cytotoxicity [112].

5. CBSIs Derived from Sources Other Than Combretastatins

5.1. Podophyllotoxin and Analogues

Podophyllotoxin (**53**, Figure 8) is a naturally occurring MTA. It binds to tubulin causing cells to accumulate in metaphase in a similar fashion to colchicine. It is the major chemical constituent of podophyllin, the alcoholic extract of the *Podophyllum* plant rhizome. These plants have long been used by indigenous populations of North America and in the Himalayas. Podophyllin was first reported in 1946 to demonstrate toxic effects against mitotic cells in similar manner to classical MTAs such as colchicine [113]; this activity was later attributed to the active component podophyllotoxin inhibiting assembly at the mitotic spindle. Despite its original promising ability to inhibit mice tumour growth and potential for translation towards treatment of human malignant tumours [114], unacceptable gastrointestinal toxicity limits its use as a chemotherapeutic agent [115].

This led to a body of work involving podophyllotoxin's optimization, culminating in semi-synthetic derivatives etoposide (**54**, Figure 8) and teniposide (**55**, Figure 8) by Sandoz Ltd. who studied glycosides of the podophyllotoxin aglycon structure. Upon condensation of benzaldehyde with the podophyllin glycoside fraction, a highly active antiproliferative agent was isolated and identified as 4'-O-demethyl-epipodophyllotoxin benzylidene-β-D-glucoside (DEPBG) (**56**, Figure 8). Condensing 4'-O-demethyl-epipodophyllotoxin glucoside led to discoveries of etoposide (**54**) and teniposide (**55**) [116]. Currently, both are licensed for the treatment of malignant tumours: etoposide for various cancers in the EU and teniposide (VUMON®) for the treatment of refractory childhood acute lymphoblastic leukaemia licensed by the FDA in the USA [117]. The mode of action of these compounds is somewhat distinct from podophyllotoxin. These compounds are known to inhibit assembly at the mitotic spindle and induce cell cycle arrest at mitosis via binding to the CBS, in addition to acting as a DNA topoisomerase II poison [118].

Continuous use of these agents remains an issue; they lead to several adverse effects including myelosuppression, acquired drug resistance, non-specific cytotoxicity and the development of secondary leukaemia [119]. The impressive anti-tumour potency and clinical efficacy of etoposide and teniposide has prompted extensive SAR studies and molecular modifications of the podophyllotoxin prototype to construct several synthetic analogues—some of which have already undergone clinical trials for various cancers but none are CSBIs. Etopophos (**57**, Figure 8) is a water-soluble phosphate (highlighted in blue, Figure 8) prodrug which has been developed by Bristol Myers and appears less toxic while more active than its parent compound [120]. It has superseded etoposide for routine clinical use [121].

5.2. Chalcones

5.2.1. Millepachine and Derivatives

The chalcone scaffold is the basis for several potent CBSIs. Chalcone combretastatin derivatives synthesised by Ducki et al. [56,57] (Figure 2) were previously discussed in Section 4.2.1. More recently, work has been carried out based on a naturally isolated chalcone named millepachine. Chalcones (58, Figure 9) are naturally occurring polyketide compounds that have been isolated from various plants. Chemically they consist of two aromatic phenyl rings joined by an $\alpha\beta$ -unsaturated enone system. They display various biological activities and in the last 25 years have emerged as an interesting class of potential anti-cancer agents. Chalcones were first recognised as cytotoxic agents in the 1970's. A series of mono and dichloro nitrochalcones was described with cytotoxic properties [122]. Chalcones were first discovered to act as potent antimetabolic agents in 1990, by Edwards et al. Their compound MDL-27048 (59, Figure 9) was effective at 4 nM in HeLa cells as a cytotoxic agent. It inhibited tubulin polymerisation in vitro at a lower concentration (1 μ M) compared to colchicine (6 μ M). Compound 59 bound rapidly with high affinity and reversibly to the tubulin heterodimer at the CBS, constituting a powerful and specific antimetabolic agent [123]. Ducki et al. have comprehensively outlined chalcones dating up to 2007 in development as promising anti-cancer agents [57]. This review will discuss more recent publications.

Milletia pachycarpa Benth (Leguminosae) is a flavonoid-rich traditional Chinese medicine which has been used as a blood tonic in anti-helminthic and as an anti-cancer preparation called 'Jixuteteng' in Chinese medicine for many years. Millepachine (60, Figure 9) is a relatively new chalcone with a 2,2-dimethylbenzopyran motif (highlighted in blue, Figure 9), isolated from the seeds of *M. pachycarpa*. Chalcone 60 has shown significant antiproliferative effects against several cancer cell lines. It has been evaluated in HepG2 tumour-bearing in vivo xenograft mice models at three concentrations and resulted in inhibition of tumour growth by 27%, 42% and 66% respectively. This compared with a 48% inhibition in mice treated solely with the control doxorubicin [124]. Poor solubility limited further dose increases and modification of 60 was necessary. Until recently 60 was characterised as a cytotoxic antimetabolic agent but the precise cellular targets were unknown. Cao et al. synthesised derivatives of millepachine which, despite targeting the CBS, appeared to stabilize tubulin in a similar fashion to docetaxel, opposing colchicine's destabilizing effect. This stabilization contradicted the paradigm of typical CBSIs as tubulin destabilizing agents [125].

Yang et al. have recently carried out biochemical and cellular experimentation, revealing through X-ray co-crystal structures of tubulin-millepachine derivatives that millepachine and derivatives were CBSIs [126]. Ring B modifications increased antiproliferative properties for millepachine derivatives. The introduction of an amino group to the B ring (61, Figure 9) increased potency by up to 253-fold in a panel of cancer cell lines from IC_{50} ranges of 1.51–4.0 μ M for parent compound millepachine (60) to an average IC_{50} of 61 to 8–26 nM for amino substituted 61. Chalcone 61 was more potent than both paclitaxel and colchicine against C26, MCF-7, HEPG2 and ES-2 cell lines. The addition of the amino at the 3-position of the B ring caused a significant increase in antiproliferative activity whereas substitution of this same amino group resulted in loss of antiproliferative activity. Molecular modelling of 61 revealed that the B ring binds deep within the CBS. The amino moiety provides an extra hydrogen bonding interaction with Val238 and stabilizes 61's interaction. This explains the greater potency of 61 in comparison to 60. Preliminary data suggests that 61 has a much lower resistance factor than paclitaxel, cisplatin and adriamycin, indicating that 60 and derivatives are unaffected by P-gp and mutant β 111 tubulin isotype expression and may be useful in treatment of refractory tumours. Compound 61 was also found to act as a potent VDA, inhibiting capillary-like tube formation in endothelial cells in concentrations as low as 50 nM. The hydrochloride salt of 61 shows promising results in in vivo models, reducing tumour growth without causing significant weight loss. In addition, 61's hydrochloride salt appears to have good oral bioavailability up to 47% [124].

Emerging research suggests that another potential mechanism of overcoming drug resistance is the design of irreversible covalent inhibitors at β -tubulin. Yang et al. found SKLB028 (**62**, Figure 9) bound irreversibly to tubulin [126]. Cells failed to recover from cell cycle arrest up to 72 h after treatment, indicating that covalent bonding had occurred. Designing anti-cancer compounds which covalently bind to their target is a well-known approach to overcome drug resistance [127,128]. Unlike the scenario in which binding is rapid, non-covalent and reversible whereby tumour cells acquire resistance by reducing target affinity or enhancing drug efflux through P-gp, MRP1 and MRP2 overexpression, resistant tumour cells cannot escape the effects of irreversible covalent binding after initial exposure to the compound.

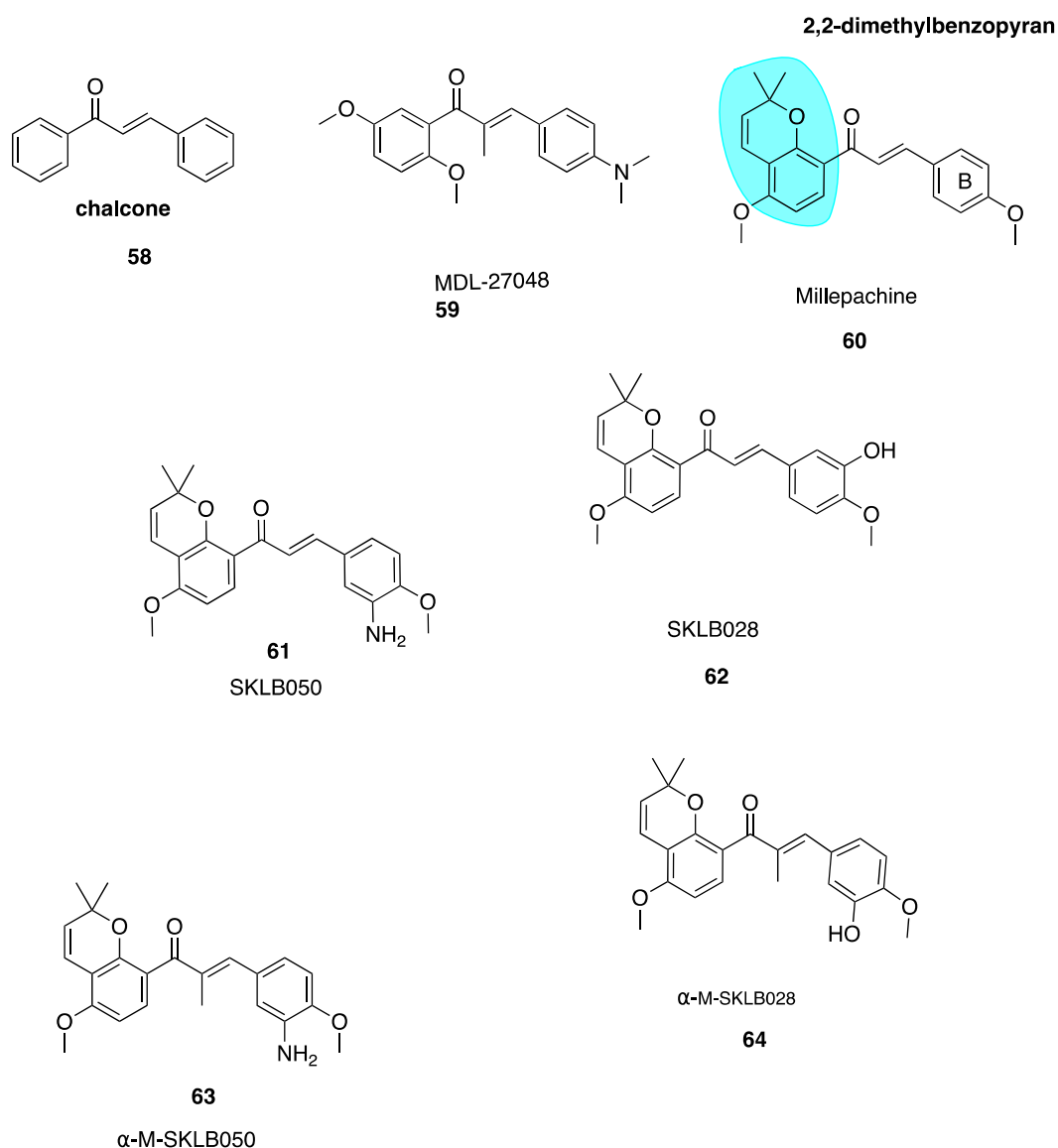


Figure 9. Structures of chalcones 58–64.

X-ray crystal structures of free millepachine compared to a co-crystal of **61** in complex with tubulin have assisted the lead optimisation process to maximise the potency of these promising derivatives. Unbound **61** adopts an *s-cis* conformation but binds into the CBS in *s-trans* configuration. Wang et al. hypothesised that an *s-trans* conformation would prove more potent. An α -methyl group was introduced to create α -M-SKLB050 (**63**, Figure 9) and α -M-SKLB028 (**64**, Figure 9). This structural change is thought to mediate *s-trans* conformations via steric repulsion that would exist between the methyl introduced and the A-ring in an *s-cis* conformation. Chalcone **63** induced cell cycle arrest at

an average concentration of 5 nM versus 24.8 nM for **61** without the additional methyl group, across five cells lines. Similarly, **64** had a promising average IC_{50} of 21 nM versus 131.5 nM for **62** [126]. These compounds have great potential as covalent inhibitors to target cancers which cannot be treated by standard, reversibly-binding MTAs.

5.2.2. New Quinolone Chalcones: CBSIs and Inhibitors of MRP1 Function

Screening of a library of compounds led to the identification of two compounds, CTR-17 (**65**, Figure 10) and CTR-20 (**66**, Figure 10), as promising lead chalcone derivatives selective for three breast cancer cell lines compared to healthy cells. Despite striking differences in structure when compared to colchicine, they appear to occupy the CBS. Compound **65** and **66** were effective in *MDR1* and *MRP1*-overexpressing MDR cells, in comparison to colchicine which was ineffective. Compound **66** is an inhibitor of the MRP1 efflux pump which contributes to its successful activity in MDR cell lines.

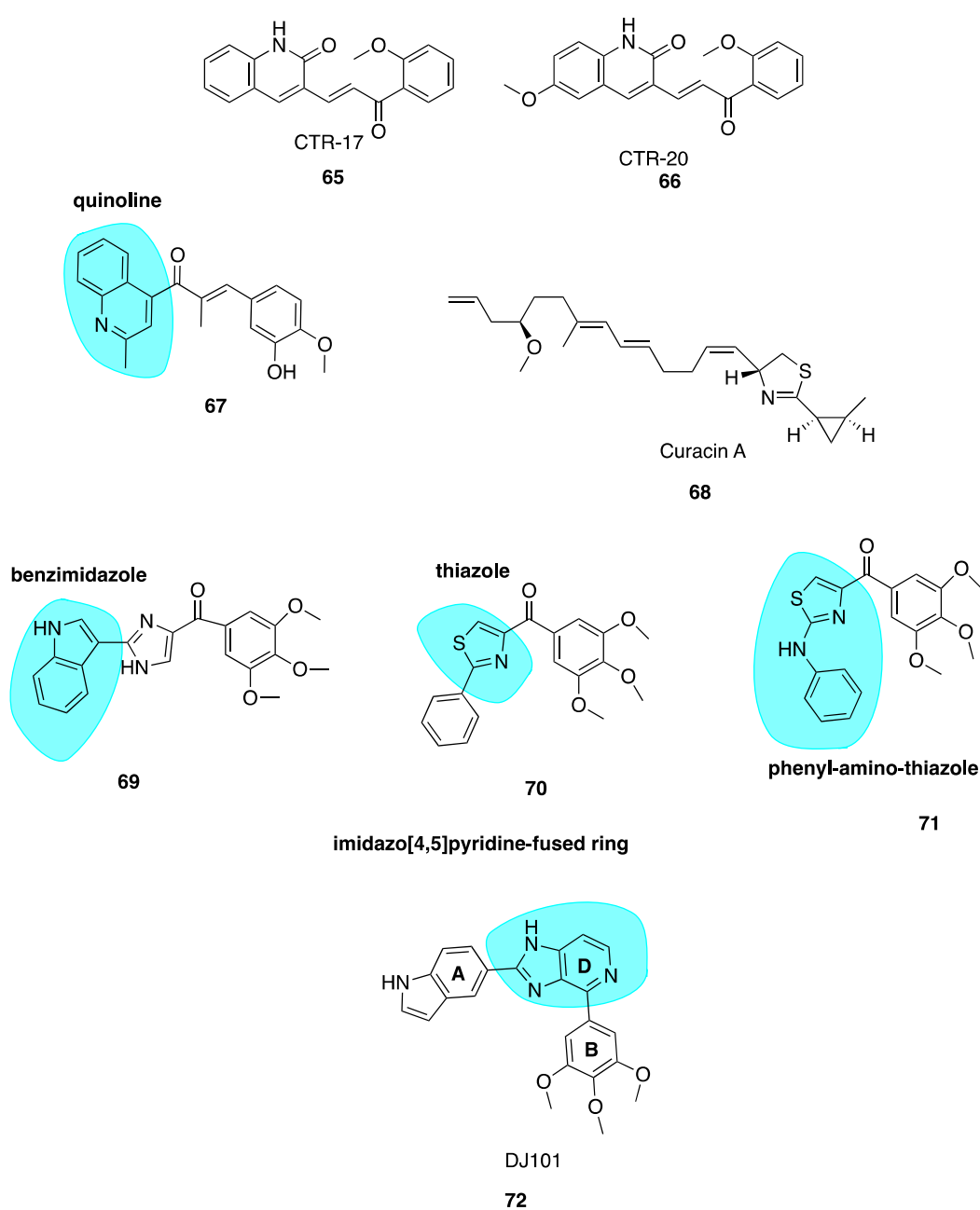


Figure 10. Structures of colchicine-binding site inhibitors 65–72.

Both compounds were extremely effective in mouse models of MDA-MB-231 triple-negative breast cancer. The treatment of mice with either **65** or **66** (30mg/kg twice a week for 30 days) successfully suppressed tumour growth. Early pre-clinical animal data is promising. Half the standard dose of paclitaxel combined with **66** proved more efficacious in animal tumours than either drug alone as a monotherapy, suggesting that this combination regimen holds potential to achieve better therapeutic results at a lower dose against MDR tumours. These lead compounds could be an excellent solution as adjunctive therapy to overcome paclitaxel's toxicity and MDR shortcomings [129].

5.2.3. Quinoline-Chalcone Derivatives of 2019

Li et al. have utilised a quinoline moiety (highlighted in blue, Figure 10) as a surrogate of CA-4's 3,4,5-trimethoxyphenyl ring with the aim of increasing aqueous solubility for clinical use, as the development of many CBSI's in the past has been limited by poor aqueous solubility [129,130]. The most potent compound of the series **67** (Figure 10) was effective in a range of cell lines with IC₅₀ values of 9 nM, in K562 human cancer cells and 15 nM in three cell lines, HEPG2, HCT8 and MDA-MB-231. It inhibited tubulin polymerisation with an IC₅₀ of 1.7 µM (CA-4: 2.5 µM), caused G₂/M arrest, depolarized mitochondria and induced reactive oxidative stress in K562 cells. Compound **67** successfully induced apoptosis by interfering with the expression of apoptotic proteins, increasing the expression of pro-apoptotic Bad and Bax proteins and downregulating the expression of anti-apoptotic Bcl-2 and Bcl-xl proteins [131].

Compound **67** appeared to be 16 more times more soluble in aqueous media than CA-4 with concentrations of 16 µg/mL attainable, likely attributable to the quinoline moiety. Additionally, the hydrochloride salt of parent compound **67** had a solubility of 1 mg/mL which is a promising starting point for modification of its physicochemical properties for use in clinic. Parent compound **67** had excellent potency in mouse liver cancer xenograft models, suppressing tumour growth by 65% with no observable toxicity. The hydrochloride salt outperformed **67** with tumour growth suppression of 69% using an identical treatment regimen. The group treated with **67** also had a much lower tumour microvessel density when compared to control, confirming the anti-vascular activity of these compounds. Compound **67** also inhibited migration and invasion of MDA-MB-231 cells, indicating potent anti-metastatic activity and potential for the treatment of resistant and aggressive triple-negative breast cancer subtypes. Collectively, this data suggests that **67** has potential for further development as an effective chemotherapeutic agent [132].

5.3. Curacin A

Curacin A (**68**, Figure 10) is the name given to a complex ketopeptide originally isolated from cyanobacterium *Lynbya majuscula*. It inhibits mitosis, tubulin polymerisation and colchicine-binding in a competitive manner through strong non-covalent binding to the CBS [132]. The structure of curacin A is unique amongst CBSIs as it lacks the recurrent aromatic moieties. Instead it bears two simple conjugated olfenic bonds [133]. Despite curacin A's excellent nanomolar antiproliferative potency in human cancer cell lines in vitro, its clinical development is hindered by high lipophilicity and therefore poor water solubility. In vivo the molecule is essentially inactive due to its water insolubility and instability [134]. Attempts have been made to synthesise superior derivatives suitable for clinical use. None appear to have advanced for further pre-clinical or clinical development at present.

5.4. Imidazo[4,5]pyridine DJ95 (DJ101)

Wei and co-workers have previously synthesised multiple series of CBSIs, with IC₅₀ values in the nanomolar range, which are highly potent against MDR cell lines. These analogues are not substrates of P-gp and thus effectively overcome P-gp-mediated resistance. The arylbenzylimidazole lead analogue ARB1-111 (**69**, Figure 10) had an average IC₅₀ of 3.8 nM and was particularly potent in melanoma and prostate cell lines [91]. Amongst the 4-substituted methoxybenzoylarylthiazole (SMART) series, compound **70** (Figure 10) was the most potent but limited by poor aqueous solubility. This was

overcome by the addition of polar groups to create the orally bioavailable phenylaminothiazole derivatives with an amino linkage between rings A and B—of which, **71** (Figure 10) was the most potent derivative. Despite excellent activities in xenograft models, the ketone moiety present in all compounds was a metabolically labile site. To block apparent *in vivo* ketone reduction, the carbonyl link was modified. A new D ring was introduced between the A and B rings to mimic the carbonyl group structure. A potent new lead compound DJ95/DJ101 (**72**, Figure 10) was identified utilising an imidazo[4,5]pyridine-fused ring template (highlighted in blue, Figure 10). This compound showed increased potency relative to parent SMART compounds with an average IC₅₀ of 5 nM in melanoma and prostate cancer cells [135].

High-resolution crystal structures of $\alpha\beta$ -tubulin in complex with **72** confirm binding at the CBS, forming three hydrogen bonds with the tubulin heterodimer [136]. Tested against NCI-60 cell lines, GI₅₀ values were less than 10 nM. *In vivo* xenograft models in A375 models of lung metastases in nude mice demonstrated 66% and 93% tumour growth inhibition at doses of 15 mg/kg and 30 mg/kg, with negligible signs of toxicity. It induced G₂/M phase cell cycle arrest with an element of vascular disruption.

Compound **72** also showed a 6.2-fold decrease in lung metastasis after two weeks in an experimental model of lung metastasis in mice. Interestingly **72** appears to be most effective in resistant tumours. *In vivo* docetaxel and paclitaxel outperformed **72** in non-resistant cell lines, with tumour growth inhibition of 101% for paclitaxel-treated mice versus 79% in **72**-treated xenograft mice. Using identical dosing schedules and frequencies in a paclitaxel resistant cell line, tumour growth inhibition was reduced by 104% by **72** versus a modest 38% using docetaxel. Therefore, **72** represents an excellent lead candidate which is effective against a broad range of resistant metastatic melanomas. Pre-clinical evaluation by Kinsie et al. supports further development as a metabolically stable, novel treatment for resistant and metastatic melanoma and other cancers. Furthermore, recently published data in 2019 evaluating **72** in ABC-transporter overexpressing cell lines concluded that this compound overcomes MDR in cancer. As with many other agents discussed in this review, it may prove an effective alternative treatment for patients when other MTAs fail to show efficacy due to acquired MDR [137].

5.5. 2-Methoxyestradiol and ENMD1198

2-Methoxyestradiol (**73**, Figure 11) is an endogenous metabolite of estradiol and is known to destabilise microtubules and have anti-angiogenic effects [138]. Compound **73** is metabolised *in vivo* via conjugation at positions 3 and 17 (highlighted in blue, Figure 11) and oxidation at position 17 to render the compound inactive. To make 2-methoxyestradiol more metabolically stable for use as a VDA, a new lead compound and CBSI ENMD-1198 (**74**, Figure 11) (Table 1) was generated by chemical modification at the C-3 and C-17 positions [139]. Of a series of analogues, **74** showed most promise and was subsequently selected as the lead compound proceeding to phase I clinical trials in 2008, in patients with refractory solid tumours as a novel antimetabolic agent, sponsored by CASI pharmaceuticals but has not yet made it to clinic. Little data has been released since 2010. Compound **74** is up to 6-fold more potent than parent compound at inhibiting endothelial cell proliferation, in addition to the potent inhibition of cell motility, tumour angiogenesis, chemotaxis and morphogenesis into capillary-like structures. It blocks vascular endothelial growth factor receptor 2 (VEGFR-2) expression in endothelial cells thus blocking endothelial cell processes involved in promoting angiogenesis. Thus, **74** is an innovative CBSI, with promising and potent anti-vascular activity [140].

Table 1. CBSIs in clinical trials and clinical use—non combretastatin A-4 analogues.

Drug Name	Section	Structural Features	Stage in Clinical Trials and Disease Treated	Company Developing Drug
ENMD1198 (74)	Section 5.5	2-Methoxyestradiol derivative	Phase I refractory solid tumours	Casi pharmaceuticals (no data published in recent years)
CP461/OSI-461 (82)	Section 5.11	Derivative of exisulind	Phase II <ul style="list-style-type: none"> Renal cell carcinoma Prostate cancer Chronic lymphocytic leukaemia (Not yet marketed or in clinical use)	Astellas
Tivantinib (86)	Section 6.2.1	Heterocyclic fused ring system	Phase II <ul style="list-style-type: none"> Hepatocellular carcinoma (HCC) Liver cancer Non-small-cell lung carcinoma (NSCLC) 	Kyowa Hakko Kirin Co. Ltd. (development discontinued in 2018 following multiple poor clinical trial outcomes)
Plinabulin (75b)	Section 6.2.2	Piperazinedione structure	Phase III stage IIIb/IV NSCLC (in combination with docetaxel)	Beyond Spring Inc.
Lisavanbulin (BAL101553) (87)	Section 6.2.3	Lysine prodrug of Avanbulin	Phase I/IIa advanced solid tumours, refractory to standard therapy	Basilea Pharmaceutica
Crolibulin (78)	Section 6.2.4	Chromene derivative	Phase I/II Clinical trials Anaplastic Thyroid Cancer	Immune Pharmaceuticals Inc; National Cancer Institute (USA) (clinical trial progression limited due to recruitment issues)

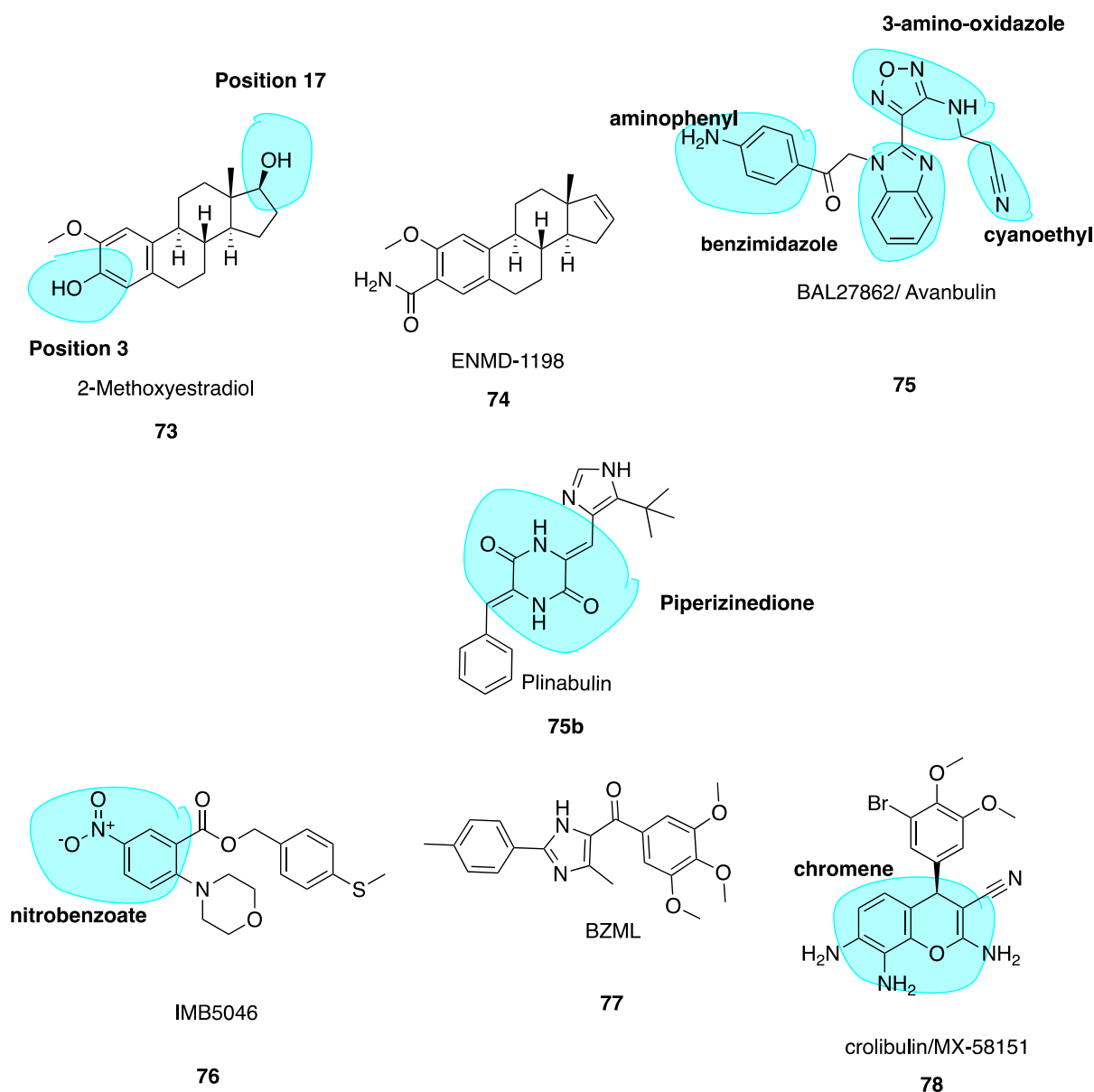


Figure 11. Structures of compounds 73–78.

5.6. Avanbulin (BAL27862) (75)

Avanbulin (BAL27862) (75, Figure 11) is a novel synthetic microtubule-targeting agent discovered via high intensity throughput optimization following high-throughput screening. It induces G₂/M phase arrest, destabilizes microtubules and has a unique microtubule-severing activity while being a potent inhibitor of tumour cell growth. It holds remarkable potency against tumour cell lines resistant to clinically relevant MTAs such as the vinca alkaloids and taxanes. In vitro, 75 demonstrated potent antiproliferative activity with a median IC₅₀ of 13.8 nM (range 5.4 nM to 25.2 nM) [141]. Despite the structural dissimilarity with colchicine, docking studies have shown that the benzimidazole and 3-amino oxadiazole moieties (highlighted in blue, Figure 11) superimpose well with C and B rings of colchicine. The cyanoethyl side chain and B ring of colchicine occupy similar binding pockets, while the aminophenyl (highlighted in blue, Figure 11) and A ring of colchicine are also in the same pocket; the amino phenyl contacts the H-7 helix of β tubulin only while colchicine's A ring interacts with H-7 and H-8 helices [20].

5.7. Nitrobenzoate IMB5046

A novel MTA 2-(4-morpholinyl)-5-nitro-benzoic acid[4-(methylthio)phenyl]methyl ester (IMB5046, **76**, Figure 11) exerts the potent inhibition of multiple tumour cells lines with an IC_{50} range of 37–400 nM. It binds to the CBS even with the absence of the traditional 3,4,5-trimethoxyphenyl moiety. Compound **76** inhibited tubulin polymerisation with an IC_{50} of 2.97 μ M. A limited proteolysis assay suggested **76** binds at the CBS. Molecular modelling studies indicated a slightly different binding mode in comparison to colchicine; hydrogen bonding to Lys254 in addition to hydrophobic interactions with Leu248 and Ala317 exclusively at the β -subunit. Compound **76**, in contrast to colchicine and other MTAs, overcame drug resistance in P-gp overexpressing KBv200 cells. Thus, **76** could act as a promising lead and novel scaffold targeting the CBS in a divergent manner when compared to other CBSIs discussed in this review [142,143].

5.8. Imidazole BZML

5-(3, 4, 5-Trimethoxybenzoyl)-4-methyl-2-(*p*-tolyl) imidazole (BZML, **77**, Figure 11), developed by Bai et al., is now in pre-clinical stages with strong cytotoxic activity and low nanomolar IC_{50} values across a family of human cancer cell lines inclusive of MDR subtypes, superior to those of CA-4. Despite striking deviations from colchicine's structure, **77** is a competitive inhibitor of colchicine at the CBS. It was found to be an irreversible modulator of P-gp function in paclitaxel-resistant lung cancer cells by decreasing P-gp expression at the protein and mRNA levels. This characteristic explains its anti-MDR properties at least in part. BZML may yet again offer another novel strategy to solve issues of drug resistance [144].

5.9. Crolibulin (MX-58151)

MX-58151 (crolibulin, **78**, Figure 11), belonging to a novel series of 2-amino-4-(3-bromo-4,5-dimethoxy-phenyl)-3-cyano-4H-chromenes (chromene highlighted in blue, Figure 11), was identified during a cell-based high throughput screening assay by Gourdeau and co-workers [145]. It was identified as a tubulin destabilizer with potent in vitro cytotoxicity specific to cancer cells as a CBSI. Compound **78** was particularly active against paclitaxel-resistant human tumour cell lines with a GI_{50} value of 2.5 nM. Renamed as crolibulin, it has been developed by EpiCept Corp. in California (Section 6.2.4 below). Crolibulin is a potent VDA with capacity to inhibit capillary tube formation at 30 nM, comparable to CA-4's value of 10 nM.

5.10. Novel Nicotinonitrile Analogues of Crolibulin and CA-4

Liu et al. recently published a series of novel 4,6-diphenyl-2-(1H-pyrrol-1-yl)nicotinonitrile analogues of crolibulin (**78**, Figure 11) and CA-4 (**2**, Figure 3) using a 2-(1H-pyrrol-1-yl)pyridine ring (highlighted in blue, **79**, Figure 12) as a link bridge in order to retain the *cis*-orientations of A and B rings. Despite crolibulin's potent pro-apoptotic and VDA activity, its neurological and cardiovascular toxicity may limit its clinical use. Consequently, efforts have been made to design novel analogues based on the crolibulin scaffold. SAR studies indicated that crolibulin's cyano group and A-ring were of utmost importance for anti-tumour action. While these moieties were retained, crolibulin's chromene structure was replaced with a phenyl substituted pyridine ring. Construction of these analogues was based on detailed SAR studies of the restricted CA-4 analogues. Considering the structural similarities required for effective CBSIs, the trimethoxyl fragment was reintroduced to ensure optimal binding to the CBS. An additional structural feature; a fluorine atom was introduced into the B-ring, further enhancing antiproliferative activity.

Several monofluorinated derivatives including **79** were over 300 times more potent than difluorinated compounds with IC_{50} values ranging from 30 nM to 310 nM across five human cancer cell lines, comparable to CA-4 and superior in potency than crolibulin. Compound **79** was more potent than CA-4 and crolibulin. The introduction of the 2-(1H-pyrrol-1-yl) pyridine in place of CA-4's double

bond not only maintained anti-tumour potency by preventing *cis-trans* isomerization but enhanced it. Molecular docking studies illustrated that **79** may bind in the CBS in a novel and superior mode, which authors note deserves further investigation [146]. Compound **79** may be advanced for further clinical evaluation based on preliminary comparative pre-clinical data between it and crolibulin [146].

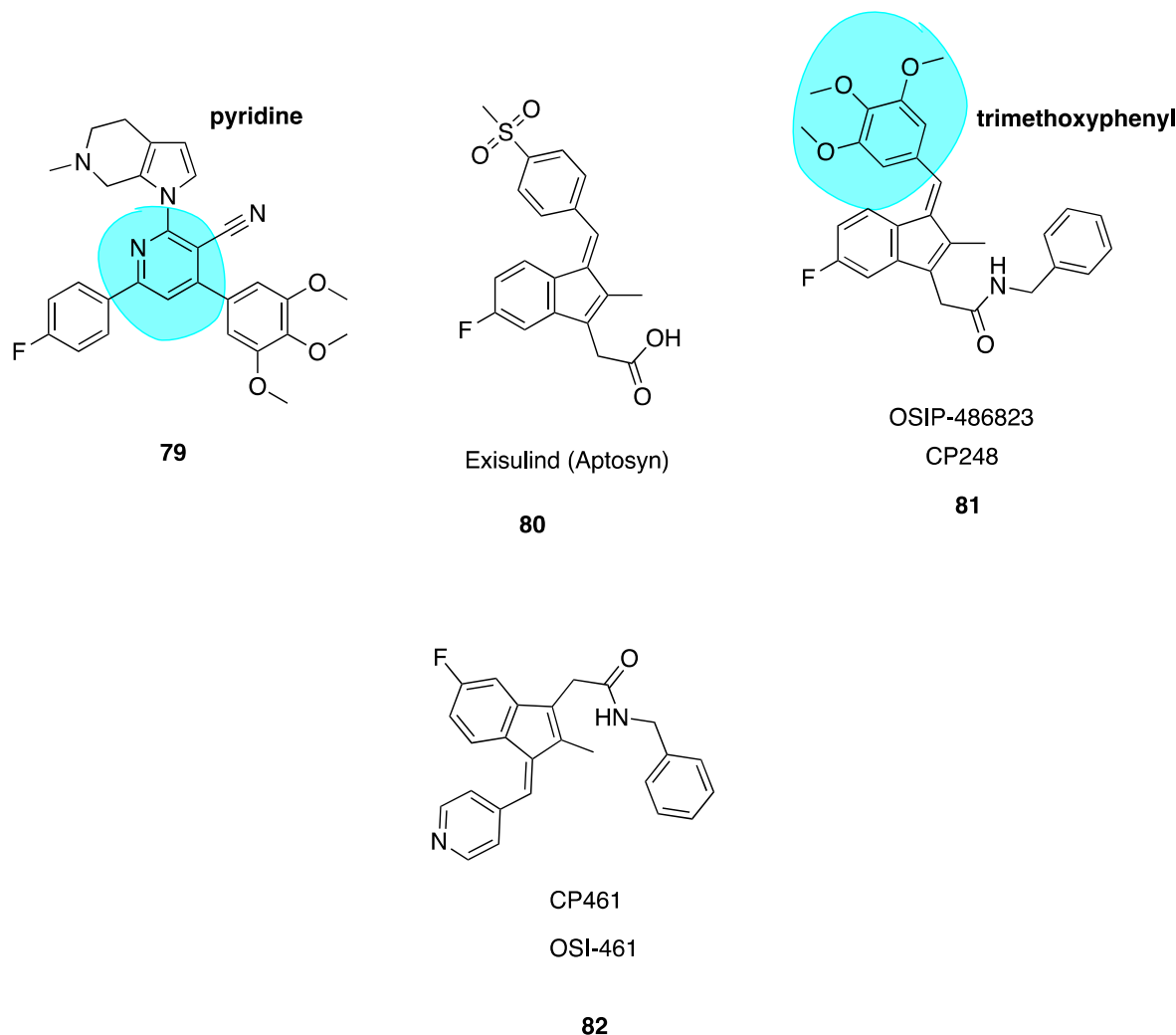


Figure 12. Crolibulin derivative **79**, exisulind, and exisulind derivatives **81–82**.

5.11. Indenes CP248 and CP461

Two potent derivatives of the pro-apoptotic sulindac-derivative exisulind (**80**, Figure 12), CP248 (also known as OSIP 486823, **81**) and CP461 (also known as OSI-461, **82**, Figure 12) (Table 1), have been found to cause growth inhibition and apoptosis in human carcinoma cell lines. Together these compounds represent a new novel class of compounds termed selective apoptotic antineoplastic drugs (SAANDS). These compounds show promise due to selective induction of apoptosis in cancerous and pre-cancerous cells. Compound **81** is an MTA, disrupting microtubule polymerisation and perturbing spindle function causing cell death in G₂/M phase. The trimethoxyphenyl group (highlighted in blue, Figure 12) of this molecule plays a role in reversible binding to the CBS, competing with colchicine likely because this portion of the molecule resembles the A ring of colchicine [147]. Compounds **81** and **82** are reported to be 100-1000-fold more potent than exisulind in terms of the inhibition of cell growth and induction of cancer cell apoptosis [148]. Compound **81** is extremely potent in colon cancer cells with an IC₅₀ value of 3 nM. Similarly, **82**, despite the absence of the trimethoxyphenyl ring structure, has similar effects on M-phase cell cycle arrest, microtubule depolymerisation and the inhibition of

mitotic spindle formation. Compound **82** appears to interact with tubulin in a different mechanism to **81** and the actual binding site remains to be determined. It has successfully undergone and is currently in various clinical trials including phase II trials for the treatment of renal cell carcinoma, prostate cancer and chronic lymphocytic leukaemia, sponsored by Astellas. The compound has yet to be marketed but it appears to have a promising future [149].

6. CBSIs in Clinical Trials and Clinical Use

6.1. Combretastatin A-4 Analogues in the Clinic

Translation of CA-4 to clinical use has been hindered by two main obstacles: isomerisation to the less potent *trans* isomer and poor water solubility. CA-4 has been an extremely attractive lead molecule for decades for the treatment of solid tumours and therefore many attempts to create diverse analogues of CA-4 are documented in the literature. The vascular damaging properties of CA-4 have prompted clinical evaluation of CA-4 phosphate derivatives (e.g., CA-4P, **83**, Figure 13). These prodrugs require chemical conversion by metabolic enzymatic processes into active pharmacological agents. Pettit et al. were the first to describe data for phosphate prodrugs of both CA-4 and CA-1 [150]. Initial attempts to synthesise prodrug derivatives of CA-4 involved the addition of a serinamide (highlighted in blue, Figure 13) to the B ring's hydroxyl group, creating an analogue known as AVE8062 (**85**, Figure 13). This CA-4 amino acid prodrug was marketed by Sanofi as ombrabulin. The serine is cleaved by aminopeptidases *in vivo* to form the active derivative [151]. The most successful prodrugs of CA-4 to date are the phosphate salt derivatives CA-4P (fosbretabulin, **83**, Figure 13) and CA-1 diphosphate (Oxi-4503, **84**, Figure 13). These prodrugs were converted to the active counterparts seven times faster in tumour and liver preparations than in blood [152]. These prodrugs are the preferred molecules for further development and clinical trials.

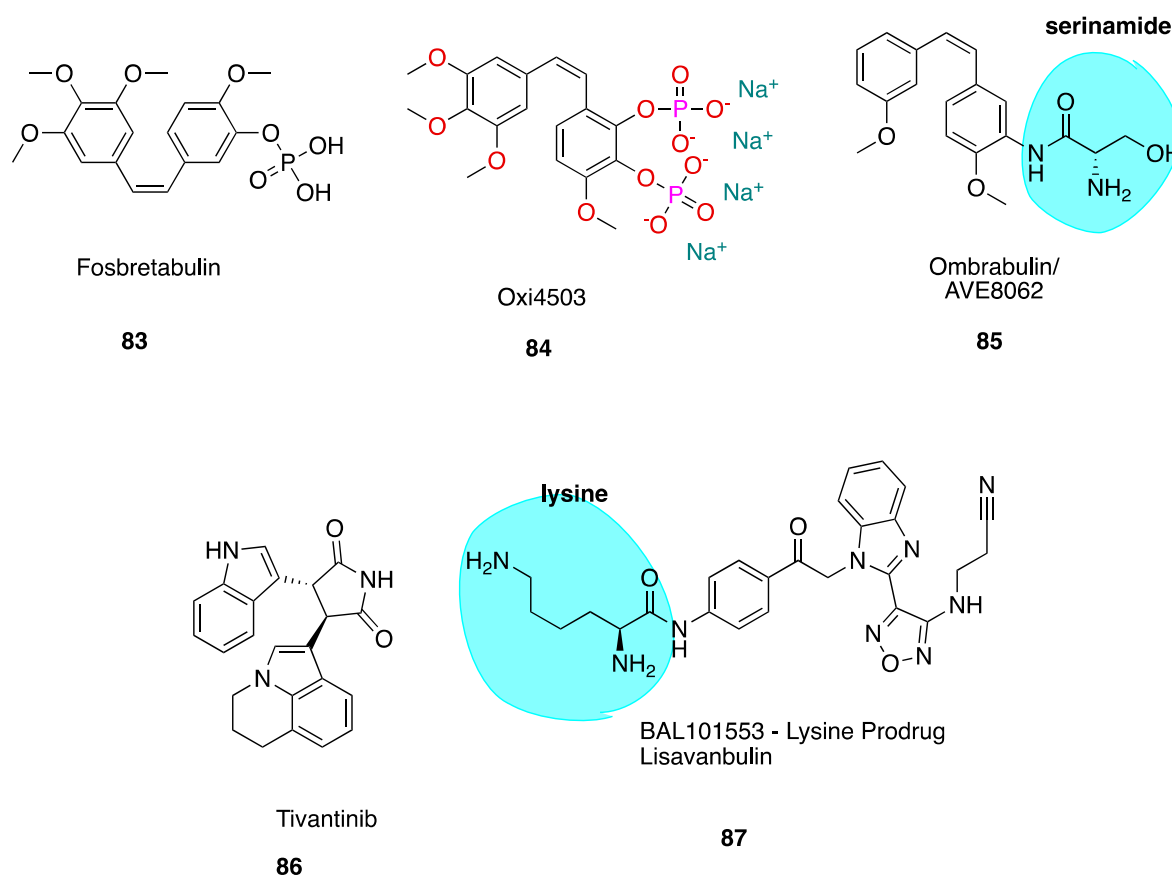


Figure 13. Structures of colchicine-binding site inhibitors in clinical trials.

6.1.1. Fosbretabulin—A CA-4 Analogue Prodrug

Several phase I/II/III clinical trials have been completed using CA-4P (fosbretabulin, **83**, Figure 13) (Table 2) for anaplastic thyroid cancer, non-small-cell lung cancers, relapsed ovarian cancer and advanced solid tumours as tumour vascular disrupting/targeting agent. It is rapidly metabolised into combretastatin after administration by non-specific endogenous phosphatases. Compound **83** has been trialled as monotherapy in clinical trials and retained its VDA in cancer patients at doses that are well tolerated. Its short half-life and reversible effects mean that it does not exhibit the traditional side-effects of tubulin-targeting and anti-angiogenic agents such as proteinuria and haemorrhage and may prolong survival in cancer patients [153]. To date, **83** has not been approved for therapeutic use due to its failure as a monotherapy, conformational instability and short half-life [154]. Due to limited success as monotherapy, further clinical evaluation is underway using **83** in combinatorial regimens with approved cancer therapies [53,54]. It has gained orphan drug status granted by the EMA in August 2013 for the treatment of ovarian cancer. At the time of designation in the EU, Diamond Biopharm Limited provide information that fosbretabulin tromethamine improved response and outcomes for platinum-resistant ovarian cancers in combination with carboplatin and paclitaxel [155]. As of March 2016, it has gained orphan drug approval for the treatment of gastro-entero-pancreatic neuroendocrine tumours. (GEP-NETS). While several products are authorised for the symptomatic management of GEP-NETS, current data shows positive results in response to fosbretabulin tromethamine [156]. Given the potential clinical success of **83** it will be exciting to see if any of the structurally modified CA-4 analogues discussed in this review make it to the clinic in the coming years.

6.1.2. Oxi4503—A CA-1 Prodrug

Oxi4503 (**84**, Figure 13) (Table 2), the diphosphate derivative of combretastatin A-1 (**3**, Figure 3), received fast-track orphan drug approval by the FDA in 2017 and is in development for the treatment of acute myeloid leukaemia (AML) by Mateon Therapeutics (formerly known as Oxigene). Despite inducing tumour necrosis, all VDAs will leave a layer of viable tumour tissue in tumour periphery, which survive due to nutritional support from normal blood vessels. This viable tumour tissue may induce rigorous and reactive angiogenesis which continues to support tumour re-growth. Combining an anti-angiogenic agent with VDA therapy may counteract this phenomenon.

Such combination therapy was trialled using the anti-angiogenic agent bevacizumab (Avastin) and **84**. A combination of bevacizumab and **84** was better than either treatment alone [40]. Treatment with **84** appears to sensitise leukaemic tumour vessels to bevacizumab. Currently, development is ongoing for the treatment of AML and myelodysplastic syndrome (MDS). It is now known that **84** targets leukaemia through a dual mechanism of action. It firstly disrupts the shape of tumour bone marrow endothelial cells in similar mechanism to regular VDAs, which in turn releases bone marrow endothelial cells. This makes them more freely available and vulnerable towards regular chemotherapeutic agents. Therefore, it holds greatest potential in combination regimens. Compound **84**, like **3**, forms an orthoquinone cytotoxic mediator in vivo which acts as a myeloperoxidase activator, directly killing tumour cells. A Phase Ib/II clinical trial, initiated in 2015, is underway investigating **84** in combination with cytarabine for treatment of MDS and AML [157].

Table 2. Summary of colchicine-binding site inhibitors (CBSIs) in clinical trials and clinical use—combretastatin A-4 analogues.

Drug Name	Section	Structural Features	Stage in Clinical Trials and Disease Treated	Company Developing Drug
Fosbretabulin (83)	Section 6.1.1	Phosphate prodrug of CA-4	Phase I/II/III <ul style="list-style-type: none"> Anaplastic thyroid NSCLC Relapsed ovarian cancer (orphan drug approval granted August 2013) Gastro-entero-pancreatic neuroendocrine tumours (GEP-NETs) (orphan drug approval granted March 2016)	Diamond Biopharm Limited
Oxi4503 (84)	Section 6.1.2	DiPhosphate prodrug of CA-1	Phase Ib/II <ul style="list-style-type: none"> acute myeloid leukaemia 	Mateon Therapeutics (previously Oxigene)
Ombrabulin/AVE8062 (85)	Section 6.1.3	Serine prodrug of CA-4	Phase II <ul style="list-style-type: none"> Ovarian cancer Advanced soft tissue sarcoma (unsuccessful—orphan drug status withdrawn)	Sanofi Aventis

6.1.3. Ombrabulin/AVE8062—An CA-4 Amino Analogue Prodrug

Another CA-4 analogue ombrabulin/AVE8062 (**85**, Figure 13) (Table 2) marketed by Sanofi Aventis with superior solubility and oral bioavailability in comparison to CA-4 has been trialled *Ombrabulin/AVE8062* in Phase 2 clinical studies for the treatment of ovarian carcinoma. It has reduced toxicity and improve anti-cancer activity relative to CA-4 [158]. It was designated orphan drug status in 2011 for the treatment of soft tissue sarcoma due to its benefit as an alternative treatment where existing protocols fail. Therapeutic synergy with cisplatin was evident in pre-clinical and phase I studies [159] and so its orphan drug approval encompasses inclusion in combination chemotherapy regimens to improve outcomes versus monotherapy alone. However, during a double-blind phase III trial for advanced soft tissue sarcoma, a progression free survival result of less than one week was considered statistically insignificant. Incremental efficacy resulted in Sanofi withdrawing orphan status and has resulted in cessation of clinical development [160].

6.2. Non-Combretastatin A-4 Analogues in Clinical Trials

6.2.1. Tivantinib

Tivantinib (**86**, Figure 13) (Table 1) was first reported as a selective oral inhibitor of MET, the tyrosine kinase receptor [161] for binding of MET to factors which promote pathways involved in tumorigenesis and metastasis [162]. It has been shown that tivantinib binds competitively with higher affinity than colchicine at the CBS pocket. Aoyoma et al. demonstrated that **86** was potent against MDR human cancer cell lines which resulted in many ongoing and completed clinical trials [163] It has been trialled in phase III trials against hepatocellular carcinoma (HCC), non-small-cell lung carcinoma (NSCLC) and liver cancer [164]. In May 2018, the results of a phase III, randomised, double-blind, placebo-controlled trial were published. Authors noted the urgent requirement for second line therapies for the treatment of HCC with overall median survival of patients being nine months and only 10% survival after five years [165]. Unfortunately, tivantinib failed to improve overall survival compared with placebo in patients with MET-high advanced HCC previously treated with sorafenib, a licensed anti-angiogenic treatment for HCC [166,167]. However, a systematic review published in 2017, which included 1824 patients from six randomized controlled trials, demonstrated that tivantinib showed significant improvement in progression free survival in solid tumours, and overall survival in particular with those patients that had high MET expression levels. Additionally, it appeared well tolerated by patients. Unfortunately, after multiple failed studies Kyowa Hakko Kirin Co. Ltd. have discontinued its development [168].

6.2.2. Plinabulin (BPI-2358, formerly NPI-2358)

Plinabulin (**75b**) (Table 1) is a small-molecule MTA and is particularly active against Kirsten rat sarcoma viral analogue homologue (KRAS)-driven cancers, which are present in 30% of cancers and are associated with poor patient survival. The effectiveness of chemotherapy is limited in KRAS-driven cancers and is often associated with toxicity [169]. Plinabulin is a non-conventional CBSI derived from marine sources. It is an analogue of halimide, an aspergillus-derived natural product MTA. Plinabulin interacts with β -tubulin as a tubulin polymerization inhibitor/de-stabilizer. Plinabulin is currently in Phase III clinical trials for the treatment of stage IIIb/IV NSCLC, pioneered by Beyond Spring Inc. in combination with docetaxel. It is being trialled in epidermal growth factor receptor (EGFR) wild-type patients, which is an under-served patient population who typically fail to respond to conventional platinum-based regimens. EGFR patients typically have shorter mean survival times of 8–10 months versus 18 months for EGFR mutant NSCLCs. Studies are ongoing and if combination therapy proves more efficacious with an improved safety profile and extended quality of life for this cohort, it holds promise to become the preferred alternative treatment where standard first line regimens fail for the treatment of NSCLC [170].

6.2.3. Lisavanbulin (BAL101553)

The amino acid lysine water-soluble prodrug of BAL27862/avanbulin (**75**, Figure 11), named lisavanbulin (also named BAL101553, **87**, Figure 13) (Table 1), is now in various clinical trials. It has completed its phase I study in adults and is now in Phase I/IIa [171].

Phase I trial results of lisavanbulin in patients with advanced solid tumours that are resistant to first line treatment indicate a loss of capillaries, suggesting that the compound has a vascular disrupting effect. Two patients of 16 demonstrated stable disease (laryngeal and rectal cancer) following > 16 cycles over 16 weeks. Results indicate that **87** is readily converted to **75** and is well tolerated at doses up to 60mg/m² while having evidence of anti-tumour activity [172]. Lisavanbulin (**87**) has undergone initial testing in a paediatric preclinical testing program (PPTP). Vincristine is the only MTA commonly used in children. Since acquired drug resistance to vincristine is a large problem in this population, it has been recognised that alternative MTAs are needed. Given the capacity to circumvent drug resistance using **87**, it was evaluated across 23 cell lines in the PPTP in vitro panel and also in vivo using PPTP solid tumour xenograft models. Unfortunately, efficacy was modest using **87** despite the parent compound having an in vitro IC₅₀ of 13.8 nM. In xenograft models only 11% of cell lines exceeded the control. The reasons for this lack of efficacy remain unclear [173]. Currently, **87** is in phase I trials in combination with radiotherapy for treating patients with newly diagnosed glioblastoma with the primary objective of determining overall progression free survival [174]. However, this amino acid prodrug is a promising emerging anti-cancer agent in clinical development, which may translate to clinical use in the coming years.

6.2.4. Crolibulin

Crolibulin (**78**, Figure 11) (Table 1) has been in Phase I/II Clinical trials since November 2010 for anaplastic thyroid cancer in combination with cisplatin. Unfortunately, the phase II trial has not yet been completed due to recruitment issues; although the compound shows potential [175].

7. Conclusions

MTAs have achieved great success in treating many diverse forms of cancer. However, acquired drug resistance over the course of treatment has become a significant limiting clinical factor with typically used agents such as the taxanes and vinca alkaloids susceptible to P-gp-mediated drug efflux. While colchicine itself cannot be used in the treatment of cancer due to systemic toxicity, several other CBSIs show promise in the future treatment of cancers of all subtypes, including those with acquired MDR characteristics. Many of these CBSIs have potent anti-angiogenic and anti-vascular activity. Hundreds of analogues with promising in vivo data targeted towards MDR cancers are known. Further progression towards clinical studies is a limiting step for many reasons, including the funding required to do so. Extensive pre-clinical studies, as outlined throughout this review, strongly suggest that CBSIs show potential to augment the use of typically used agents, thereby surmounting drug resistance mediated by P-gp, MRP1 and MRP2. Efflux pumps. There are currently a number of CBSIs in clinical trials and the results are likely to dictate the future for this drug class. It is likely that we will see new CBSIs come to the market for clinical use in the future. It is time to take CBSIs from the chemistry bench to the clinic.

Funding: This research received no external funding.

Acknowledgments: This project is supported by Trinity College Dublin's Provost's PhD Project Award awarded to NMO'B. We thank Cian O'Boyle for kindly providing images for Figures 1 and 2 and Mary J. Meegan for comments and discussions. We are grateful to the GP2A Group of Medicinal Chemists for the opportunity to contribute to this special issue.

Conflicts of Interest: NMO'B is a member of the GP2A committee.

Abbreviations

AML	Acute myeloid leukaemia
CA-1	Combretastatin A-1
CA-4	Combretastatin A-4
CA-4P	Combretastatin A-4 phosphate
CBS	Colchicine-binding site
CBSI	Colchicine-binding site inhibitor
DAMA-colchicine	N-deacetyl-N-(2-mercaptoacetyl) colchicine
DAPI	4',6-diamidino-2-phenylindole
EGFR	Epidermal growth factor receptor
FITC	Fluorescein isothiocyanate
GDP	Guanosine diphosphate
GEP-NETs	Gastro-entero-pancreatic neuroendocrine tumours
GTP	Guanosine triphosphate
HCC	Hepatocellular carcinoma
HDAC	Histone deacetylase enzyme
KRAS	Kirsten rat sarcoma viral analogue homologue
MDR	Multi-drug resistance
MDS	Myelodysplastic syndrome
MTA	Microtubule-targeting agent
NLRP3	nucleotide-binding domain (NOD)-like receptor protein
NSCLC	Non-small-cell lung carcinoma
P-gp	P-glycoprotein
PPTP	Paediatric preclinical testing program
SAR	Structure–activity relationship
UGT	UDP-glucuronyl transferase
VDA	Vascular-disrupting agent
VEGFR	Vascular endothelial growth factor receptor

References

- Adams, J. Essentials of Cell Biology. In *Learn Science at Scitable*; O'Connor, C., Ed.; NPG Education: Cambridge, UK, 2014; Available online: <https://www.nature.com/scitable/ebooks/essentials-of-cell-biology-14749010/118240354/> (accessed on 9 September 2019).
- Dominguez-Brauer, C.; Thu, K.L.; Mason, J.M.; Blaser, H.; Bray, M.R.; Mak, T.W. Targeting Mitosis in Cancer: Emerging Strategies. *Mol. Cell* **2015**, *60*, 524–536. [[CrossRef](#)]
- Downing, K.H. Structural Basis for the Interaction of Tubulin with Proteins and Drugs That Affect Microtubule Dynamics. *Ann. Rev. Cell Biol.* **2000**, *16*, 89–111. [[CrossRef](#)]
- Cooper, G.M.; Hausman, R.E.; Hausman, R.E. *The Cell: A Molecular Approach*, 2nd ed.; Sinauer Associates: Sunderland, MA, USA, 2000. Available online: <https://www.ncbi.nlm.nih.gov/books/NBK9876/> (accessed on 29 September 2019).
- Wilson, L.; Jordan, M.A. Microtubule Dynamics: Taking Aim at a Moving Target. *Chem. Biol.* **1995**, *2*, 569–573. [[CrossRef](#)]
- Rieder, C.L.; Maiato, H. Stuck in Division or Passing Through: What Happens When Cells Cannot Satisfy the Spindle Assembly Checkpoint. *Dev. Cell* **2004**, *7*, 637–651. [[CrossRef](#)] [[PubMed](#)]
- Prota, A.E.; Bargsten, K.; Diaz, J.F.; Marsh, M.; Cuevas, C.; Liniger, M.; Neuhaus, C.; Andreu, J.M.; Altmann, K.-H.; Steinmetz, M.O. A New Tubulin-Binding Site and Pharmacophore for Microtubule-Destabilizing Anticancer Drugs. *Proc. Natl. Acad. Sci. USA* **2014**, *111*, 13817–13821. [[CrossRef](#)] [[PubMed](#)]
- Maldonado, E.N.; Patnaik, J.; Mullins, M.R.; Lemasters, J.J. Free Tubulin Modulates Mitochondrial Membrane Potential in Cancer Cells. *Cancer Res.* **2010**, *70*, 10192–10201. [[CrossRef](#)] [[PubMed](#)]
- Ahern, M.J.; Reid, C.; Gordon, T.P.; McCredie, M.; Brooks, P.M.; Jones, M. Does Colchicine Work? The Results of the First Controlled Study in Acute Gout. *Aust. N. Z. J. Med.* **1987**, *17*, 301–304. [[CrossRef](#)] [[PubMed](#)]

10. Lange, U.; Schumann, C.; Schmidt, K.L. Current Aspects of Colchicine Therapy—Classical Indications and New Therapeutic Uses. *Eur. J. Med. Res.* **2001**, *6*, 150–160. [[PubMed](#)]
11. Ben-Chetrit, E.; Levy, M. Colchicine Prophylaxis in Familial Mediterranean Fever: Reappraisal after 15 Years. *Semin. Arthritis Rheum.* **1991**, *20*, 241–246. [[CrossRef](#)]
12. Yurdakul, S.; Mat, C.; Tüzün, Y.; Özyazgan, Y.; Hamuryudan, V.; Uysal, Ö.; Şenocak, M.; Yazici, H. A Double-Blind Trial of Colchicine in Behçet’s Syndrome. *Arthritis Rheum.* **2001**, *44*, 2686–2692. [[CrossRef](#)]
13. Vaidya, K.; Gonzalo Martínez, S.P. The Role of Colchicine in Acute Coronary Syndromes. *Clin. Therapeutics* **2019**, *41*, 11–20. [[CrossRef](#)] [[PubMed](#)]
14. Martinez, G.J.; Celermajer, D.S.; Patel, S. The Nlrp3 Inflammasome and the Emerging Role of Colchicine to Inhibit Atherosclerosis-Associated Inflammation. *Atherosclerosis* **2018**, *269*, 262–271. [[CrossRef](#)] [[PubMed](#)]
15. Rymer, J.A.; Newby, L.K. Failure to Launch: Targeting Inflammation in Acute Coronary Syndromes. *J. Am. Coll. Cardiol.* **2017**, *2*, 484–497.
16. Finkelstein, Y.; Aks, S.E.; Hutson, J.R.; Juurlink, D.N.; Nguyen, P.; Dubnov-Raz, G.; Pollak, U.; Koren, G.; Bentur, Y. Colchicine Poisoning: The Dark Side of an Ancient Drug. *Clin. Toxicol.* **2010**, *45*, 407–414. [[CrossRef](#)]
17. Nogales, E.; Wolf, S.G.; Downing, K.H. Structure of the Alpha-Beta Tubulin Dimer by Electron Crystallography. *Nature* **1998**, *391*, 199–204. [[CrossRef](#)]
18. Andreu, J.M.; Perez-Ramirez, B.; Gorbunoff, M.J.; Ayala, D.; Timasheff, S.N. Role of the Colchicine Ring a and Its Methoxy Groups in the Binding to Tubulin and Microtubule Inhibition. *Biochemistry* **1998**, *37*, 8356–8368. [[CrossRef](#)]
19. Ravelli, R.B.; Gigant, B.; Curmi, P.A.; Jourdain, I.; Lachkar, S.; Sobel, A.; Knossow, M. Insight into Tubulin Regulation from a Complex with Colchicine and a Stathmin-Like Domain. *Nature* **2004**, *428*, 198–202. [[CrossRef](#)]
20. Prota, A.E.; Danel, F.; Bachmann, F.; Bargsten, K.; Buey, R.M.; Pohlmann, J.; Reinelt, S.; Lane, H.; Steinmetz, M.O. The Novel Microtubule-Destabilizing Drug Bal27862 Binds to the Colchicine Site of Tubulin with Distinct Effects on Microtubule Organization. *J. Mol. Biol.* **2014**, *426*, 1848–1860. [[CrossRef](#)]
21. Dong, M.; Liu, F.; Zhou, H.; Zhai, S.; Yan, B. Novel Natural Product- and Privileged Scaffold-Based Tubulin Inhibitors Targeting the Colchicine Binding Site. *Molecules* **2016**, *21*, 1375. [[CrossRef](#)]
22. Hearn, B.R.; Shaw, S.J.; Myles, D.C. Comprehensive Medicinal Chemistry II. In *7.04 Microtubule Targeting Agents; 7.04.2.2.1 Colchicine and Analogs*; Taylor, J.B., Triggle, D.J., Eds.; 2007; Available online: <https://www.sciencedirect.com/science/article/pii/B008045044X002054> (accessed on 15 September 2019).
23. NCI National Cancer Institute. Angiogenesis Inhibitors. Available online: <https://www.cancer.gov/about-cancer/treatment/types/immunotherapy/angiogenesis-inhibitors-fact-sheet#why-is-angiogenesis-important-in-cancer> (accessed on 16 November 2019).
24. Denekamp, J. Vascular Endothelium as the Vulnerable Element in Tumours. *Acta Radiol. Oncol.* **1984**, *23*, 217–225. [[CrossRef](#)]
25. Thorpe, P.E.; Chaplin, D.J.; Blakey, D.C. The First International Conference on Vascular Targeting: Meeting Overview. *Cancer Res.* **2003**, *63*, 1144–1147. [[PubMed](#)]
26. Denekamp, J. Endothelial Cell Proliferation as a Novel Approach to Targeting Tumour Therapy. *Br. J. Cancer* **1982**, *45*, 136–139. [[CrossRef](#)]
27. Waghay, D.; Zhang, Q. Inhibit or Evade Multidrug Resistance P-Glycoprotein in Cancer Treatment. *J. Med. Chem.* **2018**, *61*, 5108–5121. [[CrossRef](#)]
28. Stengel, C.; Newman, S.P.; Leese, M.P.; Potter, B.V.L.; Reed, M.J.; Purohit, A. Class 111 Beta-Tubulin Expression and in Vitro Resistance to Microtubule Targeting Agents. *Br. J. Cancer* **2010**, *102*, 316–324. [[CrossRef](#)] [[PubMed](#)]
29. Watt, J.M.; Breyer-Brandwijk, M.G. *Medicinal Poisonous Plants Southern Eastern Africa*, 2nd ed.; Livingstone: Edinburgh, UK, 1962.
30. Kanthou, C.; Tozer, G.M. The Tumor Vascular Targeting Agent Combretastatin a-4-Phosphate Induces Reorganization of the Actin Cytoskeleton and Early Membrane Blebbing in Human Endothelial Cells. *Blood* **2002**, *99*, 2060–2069. [[CrossRef](#)]
31. Hua, J.; Sheng, Y.; Pinney, K.G.; Garner, C.M.; Kane, R.R.; Prezioso, J.A.; Pettit, G.R.; Chaplin, D.J.; Edvardsen, K. Oxi4503, a Novel Vascular Targeting Agent: Effects on Blood Flow and Antitumor Activity in Comparison to Combretastatin a-4 Phosphate. *Anticancer Res.* **2003**, *23*, 1433–1440. [[PubMed](#)]

32. Pettit, G.R.; Singh, S.B.; Hamel, E.; Lin, C.M.; Alberts, D.S.; Garcia-Kendall, D. Isolation and Structure of the Strong Cell Growth and Tubulin Inhibitor Combretastatin a-4. *Experientia* **1989**, *45*, 209–211. [[CrossRef](#)] [[PubMed](#)]
33. Siemann, D.W.; Chaplin, D.J.; Horsman, M.R. Vascular-Targeting Therapies for Treatment of Malignant Disease. *Cancer* **2004**, *100*, 2491–2499. [[CrossRef](#)]
34. McGown, A.T.; Fox, B.W. Differential Cytotoxicity of Combretastatins A1 and A4 in Two Daunorubicin-Resistant P388 Cell Lines. *Cancer Chemother. Pharmacol.* **1990**, *26*, 79–81. [[CrossRef](#)]
35. Baguley, B.C.; Holdaway, K.M.; Thomsen, L.L.; Zhuang, L.; Zwi, L.J. Inhibition of Growth of Colon 38 Adenocarcinoma by Vinblastine and Colchicine: Evidence for a Vascular Mechanism. *Eur. J. Cancer Clin. Oncol.* **1991**, *27*, 482–487. [[CrossRef](#)]
36. Hill, S.A.; Lonergan, S.J.; Denekamp, J.; Chaplin, D.J. Vinca Alkaloids: Anti-Vascular Effects in a Murine Tumour. *Eur. J. Cancer* **1993**, *29*, 1320–1324. [[CrossRef](#)]
37. Dark, G.G.; Hill, S.A.; Prise, V.E.; Tozer, G.M.; Pettit, G.R.; Chaplin, D.J. Combretastatin a-4, an Agent That Displays Potent and Selective Toxicity toward Tumor Vasculature. *Cancer Res.* **1997**, *57*, 1829–1834. [[PubMed](#)]
38. Chaplin, D.J.; Hill, S.A. The Development of Combretastatin A4 Phosphate as a Vascular Targeting Agent. *Int. J. Radiat. Oncol. Biol. Phys.* **2002**, *54*, 1491–1496. [[CrossRef](#)]
39. Kremmidiotis, G.; Leske, A.F.; Lavranos, T.C.; Beaumont, D.; Gasic, J.; Hall, A.; Callaghan, M.; Matthews, C.A.; Flynn, B. Bnc105: A Novel Tubulin Polymerization Inhibitor That Selectively Disrupts Tumor Vasculature and Displays Single-Agent Antitumor Efficacy. *Mol. Cancer Ther.* **2010**, *9*, 1562–1573. [[CrossRef](#)]
40. Siemann, D.W.; Shi, W. Dual Targeting of Tumor Vasculature: Combining Avastin and Vascular Disrupting Agents (Ca4p or Oxi4503). *Anticancer Res.* **2008**, *28*, 2027–2031.
41. Tozer, G.M.; Kanthou, C.; Lewis, G.; Prise, V.E.; Vojnovic, B.; Hill, S.A. Tumour Vascular Disrupting Agents: Combating Treatment Resistance. *Br. J. Radiol.* **2008**, *81*, 12–20. [[CrossRef](#)]
42. Pettit, G.R.; Rhodes, M.R.; Herald, D.L.; Hamel, E.; Schmidt, J.M.; Pettit, R.K. Antineoplastic Agents. 445. Synthesis and Evaluation of Structural Modifications of (Z)- and (E)-Combretastatin a-4. *J. Med. Chem.* **2005**, *48*, 4087–4099. [[CrossRef](#)]
43. Ohsumi, K.; Hatanaka, T.; Fujita, K.; Nakagawa, R.; Fukuda, Y.; Nihei, Y.; Suga, Y.; Morinaga, Y.; Akiyama, Y.; Tsuji, T. Syntheses and Antitumor Activity of Cis-Restricted Combretastatins: 5-Membered Heterocyclic Analogues. *Bioorg. Med. Chem. Lett.* **1998**, *8*, 3153–3158. [[CrossRef](#)]
44. Lee, L.; Davis, R.; Vanderham, J.; Hills, P.; Mackay, H.; Brown, T.; Mooberry, S.L.; Lee, M. 1,2,3,4-Tetrahydro-2-Thioxopyrimidine Analogs of Combretastatin-A4. *Eur. J. Med. Chem.* **2008**, *43*, 2011–2015. [[CrossRef](#)]
45. Gaspari, R.; Prota, A.E.; Bargsten, K.; Cavalli, A.; Steinmetz, M.O. Structural Basis of Cis- and Trans-Combretastatin Binding to Tubulin. *Chem* **2017**, *2*, 102–113. [[CrossRef](#)]
46. Gomtsyan, A. Heterocycles in Drugs and Drug Discovery. *Chem. Heterocycl. Compd.* **2012**, *48*, 7–10. [[CrossRef](#)]
47. Nguyen, T.T.B.; Lomberget, T.; Tran, N.C.; Colomb, E.; Nachtergaele, L.; Thoret, S.; Dubois, J.; Guillaume, J.; Abdayem, R.; Haftek, M.; et al. Synthesis and Biological Evaluation of Novel Heterocyclic Derivatives of Combretastatin a-4. *Bioorg. Med. Chem. Lett.* **2012**, *22*, 7227–7231. [[CrossRef](#)] [[PubMed](#)]
48. Herdman, C.A.; Strecker, T.E.; Tanpure, R.P.; Chen, Z.; Winters, A.; Gerberich, J.; Liu, L.; Hamel, E.; Mason, R.P.; Chaplin, D.J.; et al. Synthesis and Biological Evaluation of Benzocyclooctene-Based and Indene-Based Anticancer Agents That Function as Inhibitors of Tubulin Polymerization. *MedChemComm* **2016**, *7*, 2418–2427. [[CrossRef](#)]
49. Fürst, R.; Zupkó, I.; Berényi, Á.; Ecker, G.F.; Rinner, U. Synthesis and Antitumor-Evaluation of Cyclopropyl-Containing Combretastatin Analogs. *Bioorg. Med. Chem. Lett.* **2009**, *19*, 6948–6951. [[CrossRef](#)] [[PubMed](#)]
50. Wang, L.; Woods, K.W.; Li, Q.; Barr, K.J.; McCroskey, R.W.; Hannick, S.M.; Gherke, L.; Credo, R.B.; Hui, Y.-H.; Marsh, K.; et al. Potent, Orally Active Heterocycle-Based Combretastatin a-4 Analogues: Synthesis, Structure–Activity Relationship, Pharmacokinetics, and in Vivo Antitumor Activity Evaluation. *J. Med. Chem.* **2002**, *45*, 1697–1711. [[CrossRef](#)] [[PubMed](#)]
51. Mateo, C.; Pérez-Melero, C.; Peláez, R.; Medarde, M. Stilbenophane Analogues of Deoxycombretastatin a-4. *J. Org. Chem.* **2005**, *70*, 6544–6547. [[CrossRef](#)] [[PubMed](#)]
52. Daniel, T.; Siyaram, P.; James, M. Review of Cytotoxic Ca4 Analogues That Do Not Target Microtubules: Implications for Ca4 Development. *Mini-Rev. Med. Chem.* **2017**, *17*, 1507–1514.

53. Greene, L.M.; Meegan, M.J.; Zisterer, D.M. Combretastatins: More Than Just Vascular Targeting Agents? *J. Pharmacol. Exp. Ther.* **2015**, *355*, 212–227. [[CrossRef](#)]
54. Siemann, D.W.; Chaplin, D.J.; Walicke, P.A. A Review and Update of the Current Status of the Vasculature Disabling Agent Combretastatin-A4 Phosphate (Ca4p). *Expert Opin. Investig. Drugs* **2009**, *18*, 189–197. [[CrossRef](#)]
55. Lu, Y.; Chen, J.; Xiao, M.; Li, W.; Miller, D.D. An Overview of Tubulin Inhibitors That Interact with the Colchicine Binding Site. *Pharm. Res.* **2012**, *29*, 2943–2971. [[CrossRef](#)]
56. Ducki, S. The Development of Chalcones as Promising Anticancer Agents. *Investig. Drugs J.* **2007**, *10*, 42–46.
57. Ducki, S.; Rennison, D.; Woo, M.; Kendall, A.; Chabert, J.F.D.; McGown, A.T.; Lawrence, N.J. Combretastatin-Like Chalcones as Inhibitors of Microtubule Polymerization. Part 1: Synthesis and Biological Evaluation of Antivascular Activity. *Bioorg. Med. Chem.* **2009**, *17*, 7698–7710. [[CrossRef](#)]
58. Pettit, G.R.; Toki, B.; Herald, D.L.; Verdier-Pinard, P.; Boyd, M.R.; Hamel, E.; Pettit, R.K. Antineoplastic Agents. 379. Synthesis of Phenstatin Phosphate 1a. *J. Med. Chem.* **1998**, *41*, 1688–1695. [[CrossRef](#)] [[PubMed](#)]
59. Le Broc-Ryckewaert, D.; Pommery, N.; Pommery, J.; Ghinet, A.; Farce, A.; Wiart, J.-F.; Gautret, P.; Rigo, B.; Hénichart, J.-P. In Vitro Metabolism of Phenstatin: Potential Pharmacological Consequences. *Drug Metab. Lett.* **2011**, *5*, 209–215. [[CrossRef](#)] [[PubMed](#)]
60. Winn, B.A.; Shi, Z.; Carlson, G.J.; Wang, Y.; Nguyen, B.L.; Kelly, E.M.; Ross, R.D.T.; Hamel, E.; Chaplin, D.J.; Trawick, M.L.; et al. Bioreductively Activatable Prodrug Conjugates of Phenstatin Designed to Target Tumor Hypoxia. *Bioorg. Med. Chem. Lett.* **2017**, *27*, 636–641. [[CrossRef](#)] [[PubMed](#)]
61. Messaoudi, S.; Tréguier, B.; Hamze, A.; Provot, O.; Peyrat, J.-F.; De Losada, J.R.; Liu, J.-M.; Bignon, J.; Wdzieczak-Bakala, J.; Thoret, S.; et al. Isocombretastatins a Versus Combretastatins A: The Forgotten Isoca-4 Isomer as a Highly Promising Cytotoxic and Antitubulin Agent. *J. Med. Chem.* **2009**, *52*, 4538–4542. [[CrossRef](#)] [[PubMed](#)]
62. Zhang, L.-H.; Wu, L.; Raymon, H.K.; Chen, R.S.; Corral, L.; Shirley, M.A.; Krishna Narla, R.; Gamez, J.; Muller, G.W.; Stirling, D.I.; et al. The Synthetic Compound Cc-5079 Is a Potent Inhibitor of Tubulin Polymerization and Tumor Necrosis Factor- α Production with Antitumor Activity. *Cancer Res.* **2006**, *66*, 951–959. [[CrossRef](#)]
63. Vu, H.N.; Miller, W.J.; O'Connor, S.A.; He, M.; Schafer, P.H.; Payvandi, F.; Muller, G.W.; Stirling, D.I.; Libutti, S.K. Cc-5079: A Small Molecule with Mkp1, Antiangiogenic, and Antitumor Activity. *J. Surg. Res.* **2010**, *164*, 116–125. [[CrossRef](#)]
64. Wen, Z.; Xu, J.; Wang, Z.; Qi, H.; Xu, Q.; Bai, Z.; Zhang, Q.; Bao, K.; Wu, Y.; Zhang, W. 3-(3,4,5-Trimethoxyphenylselenyl)-1h-Indoles and Their Selenoxides as Combretastatin a-4 Analogs: Microwave-Assisted Synthesis and Biological Evaluation. *Eur. J. Med. Chem.* **2015**, *90*, 184–194. [[CrossRef](#)]
65. Zuo, D.; Guo, D.; Jiang, X.; Guan, Q.; Qi, H.; Xu, J.; Li, Z.; Yang, F.; Zhang, W.; Wu, Y. 3-(3-Hydroxy-4-Methoxyphenyl)-4-(3,4,5-Trimethoxyphenyl)-1,2,5-Selenadiazole (G-1103), a Novel Combretastatin a-4 Analog, Induces G2/M Arrest and Apoptosis by Disrupting Tubulin Polymerization in Human Cervical Hela Cells and Fibrosarcoma Ht-1080 Cells. *Chem.-Biol. Interact.* **2015**, *227*, 7–17. [[CrossRef](#)]
66. Guan, Q.; Yang, F.; Guo, D.; Xu, J.; Jiang, M.; Liu, C.; Bao, K.; Wu, Y.; Zhang, W. Synthesis and Biological Evaluation of Novel 3,4-Diaryl-1,2,5-Selenadiazol Analogues of Combretastatin a-4. *Eur. J. Med. Chem.* **2014**, *87*, 1–9. [[CrossRef](#)] [[PubMed](#)]
67. Dos Santos, E.; Hamel, E.; Bai, R.; Burnett, J.; Tozatti, C.; Bogo, D.; Perdomo, R.; Antunes, A.; Marques, M.; de Matos, M.; et al. Synthesis and Evaluation of Diaryl Sulfides and Diaryl Selenide Compounds for Antitubulin and Cytotoxic Activity. *Bioorg. Med. Chem. Lett.* **2013**, *23*, 4669–4673. [[CrossRef](#)] [[PubMed](#)]
68. Pang, Y.; An, B.; Lou, L.; Zhang, J.; Yan, J.; Huang, L.; Li, X.; Yin, S. Design, Synthesis, and Biological Evaluation of Novel Selenium-Containing Isocombretastatins and Phenstatins as Antitumor Agents. *J. Med. Chem.* **2017**, *60*, 7300–7314. [[CrossRef](#)] [[PubMed](#)]
69. Greene, T.F.; Wang, S.; Greene, L.M.; Nathwani, S.M.; Pollock, J.K.; Malebari, A.M.; McCabe, T.; Twamley, B.; O'Boyle, N.M.; Zisterer, D.M.; et al. Synthesis and Biochemical Evaluation of 3-Phenoxy-1,4-Diarylazetidins as Tubulin-Targeting Antitumor Agents. *J. Med. Chem.* **2016**, *59*, 90–113. [[CrossRef](#)]
70. Banik, I.; Becker, F.F.; Banik, B.K. Stereoselective Synthesis of B-Lactams with Polyaromatic Imines: Entry to New and Novel Anticancer Agents. *J. Med. Chem.* **2003**, *46*, 12–15. [[CrossRef](#)]

71. Sun, L.; Vasilevich, N.I.; Fuselier, J.A.; Hocart, S.J.; Coy, D.H. Examination of the 1,4-Disubstituted Azetidinone Ring System as a Template for Combretastatin a-4 Conformationally Restricted Analogue Design. *Bioorg. Med. Chem. Lett.* **2004**, *14*, 2041–2046. [[CrossRef](#)]
72. Wang, S.; Malebari, A.M.; Greene, T.F.; O'Boyle, N.M.; Fayne, D.; Nathwani, S.M.; Twamley, B.; McCabe, T.; Keely, N.O.; Zisterer, D.M.; et al. 3-Vinylazetidin-2-Ones: Synthesis, Antiproliferative and Tubulin Destabilizing Activity in Mcf-7 and Mda-Mb-231 Breast Cancer Cells. *Pharmaceuticals* **2019**, *12*, 56. [[CrossRef](#)]
73. O'Boyle, N.M.; Carr, M.; Greene, L.M.; Keely, N.O.; Knox, A.J.S.; McCabe, T.; Lloyd, D.G.; Zisterer, D.M.; Meegan, M.J. Synthesis, Biochemical and Molecular Modelling Studies of Antiproliferative Azetidinones Causing Microtubule Disruption and Mitotic Catastrophe. *Eur. J. Med. Chem.* **2011**, *46*, 4595–4607. [[CrossRef](#)]
74. O'Boyle, N.M.; Carr, M.; Greene, L.M.; Bergin, O.; Nathwani, S.M.; McCabe, T.; Lloyd, D.G.; Zisterer, D.M.; Meegan, M.J. Synthesis and Evaluation of Azetidinone Analogues of Combretastatin a-4 as Tubulin Targeting Agents. *J. Med. Chem.* **2010**, *53*, 8569–8584. [[CrossRef](#)]
75. Carr, M.; Greene, L.M.; Knox, A.J.S.; Lloyd, D.G.; Zisterer, D.M.; Meegan, M.J. Lead Identification of Conformationally Restricted B-Lactam Type Combretastatin Analogues: Synthesis, Antiproliferative Activity and Tubulin Targeting Effects. *Eur. J. Med. Chem.* **2010**, *45*, 5752–5766. [[CrossRef](#)]
76. Malebari, A.M.; Greene, L.M.; Nathwani, S.M.; Fayne, D.; O'Boyle, N.M.; Wang, S.; Twamley, B.; Zisterer, D.M.; Meegan, M.J. B-Lactam Analogues of Combretastatin a-4 Prevent Metabolic Inactivation by Glucuronidation in Chemoresistant Ht-29 Colon Cancer Cells. *Eur. J. Med. Chem.* **2017**, *130*, 261–285. [[CrossRef](#)] [[PubMed](#)]
77. Rustin, G.J.S.; Galbraith, S.M.; Anderson, H.; Stratford, M.; Folkes, L.K.; Sena, L.; Gumbrell, L.; Price, P.M. Phase I Clinical Trial of Weekly Combretastatin A4 Phosphate: Clinical and Pharmacokinetic Results. *J. Clin. Oncol.* **2003**, *21*, 2815–2822. [[CrossRef](#)] [[PubMed](#)]
78. Cummings, J.; Zelcer, N.; Allen, J.D.; Yao, D.; Boyd, G.; Maliepaard, M.; Friedberg, T.H.; Smyth, J.F.; Jodrell, D.I. Glucuronidation as a Mechanism of Intrinsic Drug Resistance in Colon Cancer Cells: Contribution of Drug Transport Proteins. *Biochem. Pharmacol.* **2004**, *67*, 31–39. [[CrossRef](#)] [[PubMed](#)]
79. Fu, D.-J.; Fu, L.; Liu, Y.-C.; Wang, J.-W.; Wang, Y.-Q.; Han, B.-K.; Li, X.-R.; Zhang, C.; Li, F.; Song, J.; et al. Structure-Activity Relationship Studies of B-Lactam-Azide Analogues as Orally Active Antitumor Agents Targeting the Tubulin Colchicine Site. *Sci. Rep.* **2017**, *7*, 12788. [[CrossRef](#)] [[PubMed](#)]
80. Macdonough, M.T.; Strecker, T.E.; Hamel, E.; Hall, J.J.; Chaplin, D.J.; Trawick, M.L.; Pinney, K.G. Synthesis and Biological Evaluation of Indole-Based, Anti-Cancer Agents Inspired by the Vascular Disrupting Agent 2-(3'-Hydroxy-4'-Methoxyphenyl)-3-(3'',4'',5''-Trimethoxybenzoyl)-6-Methoxyindole (Oxi8006). *Bioorg. Med. Chem.* **2013**, *21*, 6831–6843. [[CrossRef](#)] [[PubMed](#)]
81. Kamal, A.; Kumar, G.B.; Vishnuvardhan, M.V.P.S.; Shaik, A.B.; Reddy, V.S.; Mahesh, R.; Bin Sayeeda, I.; Kapure, J.S. Synthesis of Phenstatin/Isocombretastatin-Chalcone Conjugates as Potent Tubulin Polymerization Inhibitors and Mitochondrial Apoptotic Inducers. *Org. Biomol. Chem.* **2015**, *13*, 3963–3981. [[CrossRef](#)]
82. Maguire, C.; Chen, Z.; Mocharla, V.; Sriram, M.; Hamel, E.; Zhou, H.; Lopez, R.; Wang, Y.; Mason, R.; Chaplin, D.; et al. Synthesis of Dihydronaphthalene Analogues Inspired by Combretastatin a-4 and Their Biological Evaluation as Anticancer Agents. *MedChemComm* **2018**, *9*, 1649–1662. [[CrossRef](#)]
83. Dohle, W.; Jourdan, F.L.; Menchon, G.; Prota, A.E.; Foster, P.A.; Mannion, P.; Hamel, E.; Thomas, M.P.; Kasprzyk, P.G.; Ferrandis, E.; et al. Quinazolinone-Based Anticancer Agents: Synthesis, Antiproliferative Sar, Antitubulin Activity, and Tubulin Co-Crystal Structure. *J. Med. Chem.* **2018**, *61*, 1031–1044. [[CrossRef](#)]
84. Rastogi, S.K.; Zhao, Z.; Barrett, S.L.; Shelton, S.D.; Zafferani, M.; Anderson, H.E.; Blumenthal, M.O.; Jones, L.R.; Wang, L.; Li, X.; et al. Photoresponsive Azo-Combretastatin a-4 Analogues. *Eur. J. Med. Chem.* **2018**, *143*, 1–7. [[CrossRef](#)]
85. Sheldon, J.E.; Dcona, M.M.; Lyons, C.E.; Hackett, J.C.; Hartman, M.C.T. Photoswitchable Anticancer Activity Via Trans–Cis Isomerization of a Combretastatin a-4 Analog. *Org. Biomol. Chem.* **2016**, *14*, 40–49. [[CrossRef](#)]
86. Engdahl, A.J.; Torres, E.A.; Lock, S.E.; Engdahl, T.B.; Mertz, P.S.; Streu, C.N. Synthesis, Characterization, and Bioactivity of the Photoisomerizable Tubulin Polymerization Inhibitor Azo-Combretastatin A4. *Org. Lett.* **2015**, *17*, 4546–4549. [[CrossRef](#)] [[PubMed](#)]
87. Broichhagen, J.; Frank, J.A.; Trauner, D. A Roadmap to Success in Photopharmacology. *Acc. Chem. Res.* **2015**, *48*, 1947–1960. [[CrossRef](#)] [[PubMed](#)]
88. Velema, W.A.; Szymanski, W.; Feringa, B.L. Photopharmacology: Beyond Proof of Principle. *J. Am. Chem. Soc.* **2014**, *136*, 2178–2191. [[CrossRef](#)] [[PubMed](#)]

89. Fehrentz, T.; Schönberger, M.; Trauner, D. Optochemical Genetics. *Angew. Chem. Int. Ed.* **2011**, *50*, 12156–12182. [[CrossRef](#)]
90. Wang, Q.; Arnst, K.E.; Wang, Y.; Kumar, G.; Ma, D.; Chen, H.; Wu, Z.; Yang, J.; White, S.W.; Miller, D.D.; et al. Structural Modification of the 3,4,5-Trimethoxyphenyl Moiety in the Tubulin Inhibitor Veru-111 Leads to Improved Antiproliferative Activities. *J. Med. Chem.* **2018**, *61*, 7877–7891. [[CrossRef](#)] [[PubMed](#)]
91. Chen, J.; Ahn, S.; Wang, J.; Lu, Y.; Dalton, J.T.; Miller, D.D.; Li, W. Discovery of Novel 2-Aryl-4-Benzoyl-Imidazole (Abi-Iii) Analogues Targeting Tubulin Polymerization as Antiproliferative Agents. *J. Med. Chem.* **2012**, *55*, 7285–7289. [[CrossRef](#)]
92. Chen, J.; Li, C.-M.; Wang, J.; Ahn, S.; Wang, Z.; Lu, Y.; Dalton, J.T.; Miller, D.D.; Li, W. Synthesis and Antiproliferative Activity of Novel 2-Aryl-4-Benzoyl-Imidazole Derivatives Targeting Tubulin Polymerization. *Bioorg. Med. Chem.* **2011**, *19*, 4782–4795. [[CrossRef](#)]
93. Kashyap, V.K.; Wang, Q.; Setua, S.; Nagesh, P.K.B.; Chauhan, N.; Kumari, S.; Chowdhury, P.; Miller, D.D.; Yallapu, M.M.; Li, W.; et al. Therapeutic Efficacy of a Novel Biii/Biv-Tubulin Inhibitor (Veru-111) in Pancreatic Cancer. *J. Exp. Clin. Cancer Res.* **2019**, *38*, 29. [[CrossRef](#)]
94. Hwang, D.-J.; Wang, J.; Li, W.; Miller, D.D. Structural Optimization of Indole Derivatives Acting at Colchicine Binding Site as Potential Anticancer Agents. *ACS Med. Chem. Lett.* **2015**, *6*, 993–997. [[CrossRef](#)]
95. Wang, Q.; Arnst, K.E.; Wang, Y.; Kumar, G.; Ma, D.; White, S.W.; Miller, D.D.; Li, W.; Li, W. Structure-Guided Design, Synthesis, and Biological Evaluation of (2-(1h-Indol-3-Yl)-1h-Imidazol-4-Yl)(3,4,5-Trimethoxyphenyl) Methanone (Abi-231) Analogues Targeting the Colchicine Binding Site in Tubulin. *J. Med. Chem.* **2019**, *62*, 6734–6750. [[CrossRef](#)]
96. Romagnoli, R.; Baraldi, P.G.; Salvador, M.K.; Preti, D.; Aghazadeh Tabrizi, M.; Brancale, A.; Fu, X.-H.; Li, J.; Zhang, S.-Z.; Hamel, E.; et al. Synthesis and Evaluation of 1,5-Disubstituted Tetrazoles as Rigid Analogues of Combretastatin a-4 with Potent Antiproliferative and Antitumor Activity. *J. Med. Chem.* **2012**, *55*, 475–488. [[CrossRef](#)] [[PubMed](#)]
97. Romagnoli, R.; Oliva, P.; Salvador, M.K.; Camacho, M.E.; Padroni, C.; Brancale, A.; Ferla, S.; Hamel, E.; Ronca, R.; Grillo, E.; et al. Design, Synthesis and Biological Evaluation of Novel Vicinal Diaryl-Substituted 1h-Pyrazole Analogues of Combretastatin a-4 as Highly Potent Tubulin Polymerization Inhibitors. *Eur. J. Med. Chem.* **2019**, *181*, 111577. [[CrossRef](#)] [[PubMed](#)]
98. Sánchez Maya, A.B.; Pérez-Melero, C.; Salvador, N.; Peláez, R.; Caballero, E.; Medarde, M. New Naphthylcombretastatins. Modifications on the Ethylene Bridge. *Bioorg. Med. Chem.* **2005**, *13*, 2097–2107. [[CrossRef](#)] [[PubMed](#)]
99. Dupuis, M.L.; Flego, M.; Molinari, A.; Cianfriglia, M. Saquinavir Induces Stable and Functional Expression of the Multidrug Transporter P-Glycoprotein in Human Cd4 T-Lymphoblastoid Cemrev Cells. *HIV Med.* **2003**, *4*, 338–345. [[CrossRef](#)]
100. Lai, Q.; Wang, Y.; Wang, R.; Lai, W.; Tang, L.; Tao, Y.; Liu, Y.; Zhang, R.; Huang, L.; Xiang, H.; et al. Design, Synthesis and Biological Evaluation of a Novel Tubulin Inhibitor 7a3 Targeting the Colchicine Binding Site. *Eur. J. Med. Chem.* **2018**, *156*, 162–179. [[CrossRef](#)]
101. O'Boyle, N.M.; Ana, G.; Kelly, P.M.; Nathwani, S.M.; Noorani, S.; Fayne, D.; Bright, S.A.; Twamley, B.; Zisterer, D.M.; Meegan, M.J. Synthesis and Evaluation of Antiproliferative Microtubule-Destabilising Combretastatin A-4 Piperazine Conjugates. *Org. Biomol. Chem.* **2019**, *17*, 6184–6200. [[CrossRef](#)]
102. Choi, J.-H.; Kwon, H.J.; Yoon, B., II; Kim, J.-H.; Han, S.U.; Joo, H.J.; Kim, D.-Y. Expression Profile of Histone Deacetylase 1 in Gastric Cancer Tissues. *Jpn. J. Cancer Res.* **2001**, *92*, 1300–1304. [[CrossRef](#)]
103. Boyle, N.M.O.; Meegan, M.J. Designed Multiple Ligands for Cancer Therapy. *Curr. Med. Chem.* **2011**, *18*, 4722–4737. [[CrossRef](#)]
104. Schmitt, F.; Gosch, L.C.; Dittmer, A.; Rothemund, M.; Mueller, T.; Schobert, R.; Biersack, B.; Volkamer, A.; Höpfner, M. Oxazole-Bridged Combretastatin a-4 Derivatives with Tethered Hydroxamic Acids: Structure-Activity Relations of New Inhibitors of Hdac and/or Tubulin Function. *Int. J. Mol. Sci.* **2019**, *20*, 383. [[CrossRef](#)]
105. Khelifi, I.; Naret, T.; Renko, D.; Hamze, A.; Bernadat, G.; Bignon, J.; Lenoir, C.; Dubois, J.; Brion, J.-D.; Provot, O.; et al. Design, Synthesis and Anticancer Properties of Isocombretaquinolines as Potent Tubulin Assembly Inhibitors. *Eur. J. Med. Chem.* **2017**, *127*, 1025–1034. [[CrossRef](#)]

106. Patil, R.; Patil, S.A.; Beaman, K.D.; Patil, S.A. Indole Molecules as Inhibitors of Tubulin Polymerization: Potential New Anticancer Agents, an Update (2013–2015). *Future Med. Chem.* **2016**, *8*, 1291–1316. [[CrossRef](#)] [[PubMed](#)]
107. Patil, S.A.; Patil, R.; Miller, D.D. Indole Molecules as Inhibitors of Tubulin Polymerization: Potential New Anticancer Agents. *Future Med. Chem.* **2012**, *4*, 2085–2115. [[CrossRef](#)] [[PubMed](#)]
108. Brancale, A.; Silvestri, R. Indole, a Core Nucleus for Potent Inhibitors of Tubulin Polymerization. *Med. Res. Rev.* **2007**, *27*, 209–238. [[CrossRef](#)] [[PubMed](#)]
109. Li, W.; Shuai, W.; Sun, H.; Xu, F.; Bi, Y.; Xu, J.; Ma, C.; Yao, H.; Zhu, Z.; Xu, S. Design, Synthesis and Biological Evaluation of Quinoline-Indole Derivatives as Anti-Tubulin Agents Targeting the Colchicine Binding Site. *Eur. J. Med. Chem.* **2019**, *163*, 428–442. [[CrossRef](#)]
110. Naret, T.; Khelifi, I.; Provot, O.; Bignon, J.; Levaique, H.; Dubois, J.; Souce, M.; Kassalouri, A.; Deroussent, A.; Paci, A.; et al. 1,1-Diheterocyclic Ethylenes Derived from Quinaldine and Carbazole as New Tubulin-Polymerization Inhibitors: Synthesis, Metabolism, and Biological Evaluation. *J. Med. Chem.* **2019**, *62*, 1902–1916. [[CrossRef](#)]
111. Niu, H.; Strecker, T.E.; Gerberich, J.L.; Campbell, J.W.; Saha, D.; Mondal, D.; Hamel, E.; Chaplin, D.J.; Mason, R.P.; Trawick, M.L.; et al. Structure Guided Design, Synthesis, and Biological Evaluation of Novel Benzosuberene Analogues as Inhibitors of Tubulin Polymerization. *J. Med. Chem.* **2019**, *62*, 5594–5615. [[CrossRef](#)]
112. Mustafa, M.; Anwar, S.; Elgamal, F.; Ahmed, E.R.; Aly, O.M. Potent Combretastatin a-4 Analogs Containing 1,2,4-Triazole: Synthesis, Antiproliferative, Anti-Tubulin Activity, and Docking Study. *Eur. J. Med. Chem.* **2019**, *183*, 111697. [[CrossRef](#)]
113. King, M.L.S.; Sullivan, M.M. The Similarity of the Effect of Podophyllin and Colchicine and Their Use in the Treatment of Condylomata Acuminata. *Science* **1946**, *104*, 244–245. [[CrossRef](#)]
114. Kern, A.B.; Fanger, H. Podophyllin in the Treatment of Cutaneous Carcinoma. *JAMA Dermatol.* **1950**, *62*, 526–532. [[CrossRef](#)] [[PubMed](#)]
115. Canel, C.; Moraes, R.M.; Dayan, F.E.; Ferreira, D. Podophyllotoxin. *Phytochemistry* **2000**, *54*, 115–120. [[CrossRef](#)]
116. Stähelin, H.F.; von Wartburg, A. The Chemical and Biological Route from Podophyllotoxin Glucoside to Etoposide: Ninth Cain Memorial Award Lecture. *Cancer Res.* **1991**, *51*, 5–15. [[PubMed](#)]
117. FDA Vumon®(Teniposide Injection). Available online: https://www.accessdata.fda.gov/drugsatfda_docs/label/2011/020119s010s011bl.pdf (accessed on 24 December 2019).
118. Duca, M.; Guianvarc'h, D.; Meresse, P.; Bertounesque, E.; Dauzonne, D.; Kraus-Berthier, L.; Thiot, S.; Léonce, S.; Pierré, A.; Pfeiffer, B.; et al. Synthesis and Biological Study of a New Series of 4'-Demethylepipodophyllotoxin Derivatives. *J. Med. Chem.* **2005**, *48*, 593–603. [[CrossRef](#)] [[PubMed](#)]
119. Keating, G.M. Rituximab: A Review of Its Use in Chronic Lymphocytic Leukaemia, Low-Grade or Follicular Lymphoma and Diffuse Large B-Cell Lymphoma. *Drugs* **2010**, *70*, 1445–1476. [[CrossRef](#)] [[PubMed](#)]
120. Saulnier, M.G.; Langley, D.R.; Kadow, J.F.; Senter, P.D.; Knipe, J.O.; Tun, M.M.; Vyas, D.M.; Doyle, T.W. Synthesis of Etoposide Phosphate, Bmy-40481: A Water-Soluble Clinically Active Prodrug of Etoposide. *Bioorg. Med. Chem. Lett.* **1994**, *4*, 2567–2572. [[CrossRef](#)]
121. Hande, K.R. Etoposide: Four Decades of Development of a Topoisomerase II Inhibitor. *Eur. J. Cancer* **1998**, *34*, 1514–1521. [[CrossRef](#)]
122. Doré, J.; Viel, C. Antitumor Chemotherapy. IX. Cytotoxic Activity in Cultured Tumor Cells of Chalcone Substituents and Related Compounds. *Journal de Pharmacie de Belgique* **1974**, *29*, 341.
123. Peyrot, V.; Leynadier, D.; Sarrazin, M.; Briand, C.; Menendez, M.; Laynez, J.; Andreu, J.M. Mechanism of Binding of the New Antimitotic Drug Mdl 27048 to the Colchicine Site of Tubulin: Equilibrium Studies. *Biochemistry* **1992**, *31*, 11125–11132. [[CrossRef](#)]
124. Yang, Z.; Wu, W.; Wang, J.; Liu, L.; Li, L.; Yang, J.; Wang, G.; Cao, D.; Zhang, R.; Tang, M.; et al. Synthesis and Biological Evaluation of Novel Millepachine Derivatives as a New Class of Tubulin Polymerization Inhibitors. *J. Med. Chem.* **2014**, *57*, 7977–7989. [[CrossRef](#)]
125. Cao, D.; Han, X.; Wang, G.; Yang, Z.; Peng, F.; Ma, L.; Zhang, R.; Ye, H.; Tang, M.; Wu, W.; et al. Synthesis and Biological Evaluation of Novel Pyranochalcone Derivatives as a New Class of Microtubule Stabilizing Agents. *Eur. J. Med. Chem.* **2013**, *62*, 579–589. [[CrossRef](#)]

126. Yang, J.; Yan, W.; Yu, Y.; Wang, Y.; Yang, T.; Xue, L.; Yuan, X.; Long, C.; Liu, Z.; Chen, X.; et al. The Compound Millepachine and Its Derivatives Inhibit Tubulin Polymerization by Irreversibly Binding to the Colchicine-Binding Site in β -Tubulin. *J. Biol. Chem.* **2018**, *293*, 9461–9472. [[CrossRef](#)]
127. Engel, J.; Lategahn, J.; Rauh, D. Hope and Disappointment: Covalent Inhibitors to Overcome Drug Resistance in Non-Small Cell Lung Cancer. *ACS Med. Chem. Lett.* **2015**, *7*, 2–5. [[CrossRef](#)] [[PubMed](#)]
128. Tan, L.; Wang, J.; Tanizaki, J.; Huang, Z.; Aref, A.R.; Rusan, M.; Zhu, S.-J.; Zhang, Y.; Ercan, D.; Liao, R.G.; et al. Development of Covalent Inhibitors That Can Overcome Resistance to First-Generation Fgfr Kinase Inhibitors. *Proc. Natl. Acad. Sci. USA* **2014**, *111*, 4869–4877. [[CrossRef](#)] [[PubMed](#)]
129. Lindamulage, I.K.; Vu, H.-Y.; Karthikeyan, C.; Knockleby, J.; Lee, Y.-F.; Trivedi, P.; Lee, H. Novel Quinolone Chalcones Targeting Colchicine-Binding Pocket Kill Multidrug-Resistant Cancer Cells by Inhibiting Tubulin Activity and Mrp1 Function. *Sci. Rep.* **2017**, *7*, 10298. [[CrossRef](#)] [[PubMed](#)]
130. O'Boyle, N.M.; Greene, L.M.; Keely, N.O.; Wang, S.; Cotter, T.S.; Zisterer, D.M.; Meegan, M.J. Synthesis and Biochemical Activities of Antiproliferative Amino Acid and Phosphate Derivatives of Microtubule-Disrupting β -Lactam Combretastatins. *Eur. J. Med. Chem.* **2013**, *62*, 705–721. [[CrossRef](#)] [[PubMed](#)]
131. Moldoveanu, T.; Follis, A.V.; Kriwacki, R.W.; Green, D.R. Many Players in Bcl-2 Family Affairs. *Trends Biochem. Sci.* **2014**, *39*, 101–111. [[CrossRef](#)] [[PubMed](#)]
132. Li, W.; Xu, F.; Shuai, W.; Sun, H.; Yao, H.; Ma, C.; Xu, S.; Yao, H.; Zhu, Z.; Yang, D.-H.; et al. Discovery of Novel Quinolone–Chalcone Derivatives as Potent Antitumor Agents with Microtubule Polymerization Inhibitory Activity. *J. Med. Chem.* **2019**, *62*, 993–1013. [[CrossRef](#)]
133. Hamel, E. Antimitotic Natural Products and Their Interactions with Tubulin. *Med. Res. Rev.* **1996**, *16*, 207–231. [[CrossRef](#)]
134. Wipf, P.; Reeves, J.T.; Day, B.W. Chemistry and Biology of Curacin, A. *Curr. Pharm. Des.* **2004**, *10*, 1417–1437. [[CrossRef](#)]
135. Lu, Y.; Li, C.-M.; Wang, Z.; Chen, J.; Mohler, M.L.; Li, W.; Dalton, J.T.; Miller, D.D. Design, Synthesis, and SAR Studies of 4-Substituted Methoxylbenzoyl-Aryl-Thiazoles Analogues as Potent and Orally Bioavailable Anticancer Agents. *J. Med. Chem.* **2011**, *54*, 4678–4693. [[CrossRef](#)]
136. RCSB 6NNG Tubulin-Rb3_Sld-Ttl in Complex with Compound DJ95. Available online: <https://www.rcsb.org/structure/6NNG> (accessed on 10 November 2019).
137. Arnst, K.E.; Wang, Y.; Lei, Z.-N.; Hwang, D.-J.; Kumar, G.; Ma, D.; Parke, D.N.; Chen, Q.; Yang, J.; White, S.W.; et al. Colchicine Binding Site Agent Dj95 Overcomes Drug Resistance and Exhibits Antitumor Efficacy. *Mol. Pharmacol.* **2019**, *96*, 73–89. [[CrossRef](#)]
138. Matei, D.; Schilder, J.; Sutton, G.; Perkins, S.; Breen, T.; Quon, C.; Sidor, C. Activity of 2-Methoxyestradiol (Panzem[®] Ncd) in Advanced, Platinum-Resistant Ovarian Cancer and Primary Peritoneal Carcinomatosis: A Hoosier Oncology Group Trial. *Gynecol. Oncol.* **2009**, *115*, 90–96. [[CrossRef](#)] [[PubMed](#)]
139. LaVallee, T.M.; Burke, P.A.; Swartz, G.M.; Hamel, E.; Agoston, G.E.; Shah, J.; Suwandi, L.; Hanson, A.D.; Fogler, W.E.; Sidor, C.F.; et al. Significant Antitumor Activity In Vivo Following Treatment with the Microtubule Agent Enmd-1198. *Mol. Cancer Ther.* **2008**, *7*, 1472–1482. [[CrossRef](#)] [[PubMed](#)]
140. Pasquier, E.; Sinnappan, S.; Munoz, M.A.; Kavallaris, M. Enmd-1198, a New Analogue of 2-Methoxyestradiol, Displays Both Antiangiogenic and Vascular-Disrupting Properties. *Mol. Cancer Ther.* **2010**, *9*, 1408–1418. [[CrossRef](#)] [[PubMed](#)]
141. Esteve, M.-A.; Honore, S.; McKay, N.; Bachmann, F.; Lane, H.; Braguer, D. Abstract 1977: Bal27862: A Unique Microtubule-Targeted Drug That Suppresses Microtubule Dynamics, Severs Microtubules, and Overcomes Bcl-2- and Tubulin Subtype-Related Drug Resistance. *Cancer Res.* **2010**, *70*, 1977.
142. Zheng, S.; Zhong, Q.; Mottamal, M.; Zhang, Q.; Zhang, C.; LeMelle, E.; McFerrin, H.; Wang, G. Design, Synthesis, and Biological Evaluation of Novel Pyridine-Bridged Analogues of Combretastatin-A4 as Anticancer Agents. *J. Med. Chem.* **2014**, *57*, 3369–3381. [[CrossRef](#)] [[PubMed](#)]
143. Zheng, Y.-B.; Gong, J.-H.; Liu, X.-J.; Wu, S.-Y.; Li, Y.; Xu, X.-D.; Shang, B.-Y.; Zhou, J.-M.; Zhu, Z.-L.; Si, S.-Y.; et al. A Novel Nitrobenzoate Microtubule Inhibitor That Overcomes Multidrug Resistance Exhibits Antitumor Activity. *Sci. Rep.* **2016**, *6*, 31472. [[CrossRef](#)]
144. Bai, Z.; Gao, M.; Zhang, H.; Guan, Q.; Xu, J.; Li, Y.; Qi, H.; Li, Z.; Zuo, D.; Zhang, W.; et al. BZML, a Novel Colchicine Binding Site Inhibitor, Overcomes Multidrug Resistance in A549/Taxol Cells by Inhibiting P-Gp Function and Inducing Mitotic Catastrophe. *Cancer Lett.* **2017**, *402*, 81–92. [[CrossRef](#)]

145. Gourdeau, H.; Leblond, L.; Hamelin, B.; Desputeau, C.; Dong, K.; Kianicka, I.; Custeau, D.; Boudreau, C.; Geerts, L.; Cai, S.-X.; et al. Antivascular and Antitumor Evaluation of 2-Amino-4-(3-Bromo-4,5-Dimethoxy-Phenyl)-3-Cyano-4-Chromenes, a Novel Series of Anticancer Agents. *Mol. Cancer Ther.* **2004**, *3*, 1375–1384.
146. Liu, Y.; Yang, D.; Hong, Z.; Guo, S.; Liu, M.; Zuo, D.; Ge, D.; Qin, M.; Sun, D. Synthesis and Biological Evaluation of 4,6-Diphenyl-2-(1h-Pyrrol-1-Yl)Nicotinonitrile Analogues of Crolibulin and Combretastatin a-4. *Eur. J. Med. Chem.* **2018**, *146*, 185–193. [[CrossRef](#)]
147. Xiao, D.; Deguchi, A.; Gundersen, G.G.; Oehlen, B.; Arnold, L.; Weinstein, I.B. The Sulindac Derivatives Osi-461, Osip486823, and Osip487703 Arrest Colon Cancer Cells in Mitosis by Causing Microtubule Depolymerization. *Mol. Cancer Ther.* **2006**, *5*, 60–67. [[CrossRef](#)]
148. Haanen, C. Sulindac and Its Derivatives: A Novel Class of Anticancer Agents. *Curr. Opin. Investig. Drugs* **2001**, *2*, 677–683. [[PubMed](#)]
149. Clinicaltrials Gov. 6 Studies Found For: CP 461/Osi-461. Available online: <https://clinicaltrials.gov/ct2/results?cond=&term=CP+461&cntry=&state=&city=&dist=> (accessed on 19 September 2019).
150. Pettit, G.R.; Lippert, J.W. Antineoplastic Agents 429. Syntheses of the Combretastatin a-1 and Combretastatin B-1 Prodrugs. *Anti-Cancer Drug Des.* **2000**, *15*, 203–216.
151. Tozer, G.M.; Kanthou, C.; Parkins, C.S.; Hill, S.A. The Biology of the Combretastatins as Tumour Vascular Targeting Agents. *Int. J. Exp. Pathol.* **2002**, *83*, 21–38. [[CrossRef](#)] [[PubMed](#)]
152. Kirwan, I.G.; Loadman, P.M.; Swaine, D.J.; Anthoney, D.A.; Pettit, G.R.; Lippert, J.W.; Shnyder, S.D.; Cooper, P.A.; Bibby, M.C. Comparative Preclinical Pharmacokinetic and Metabolic Studies of the Combretastatin Prodrugs Combretastatin A4 Phosphate and A1 Phosphate. *Clin. Cancer Res.* **2004**, *10*, 1446–1453. [[CrossRef](#)] [[PubMed](#)]
153. Mooney, C.J.; Nagaiah, G.; Fu, P.; Wasman, J.K.; Cooney, M.M.; Savvides, P.S.; Bokar, J.A.; Dowlati, A.; Wang, D.; Agarwala, S.S.; et al. A Phase II Trial of Fosbretabulin in Advanced Anaplastic Thyroid Carcinoma and Correlation of Baseline Serum-Soluble Intracellular Adhesion Molecule-1 with Outcome. *Thyroid* **2009**, *19*, 233–240. [[CrossRef](#)] [[PubMed](#)]
154. Griggs, M.J.; Hesketh, R. Targeting Tumour Vasculature: The Development of Combretastatin A4. *Lancet Oncol.* **2001**, *2*, 82–87. [[CrossRef](#)]
155. EMA. *Public Summary of Opinion on Orphan Designation; Fosbretabulin Tromethamine for the Treatment of Gastro-Entero-Pancreatic Neuroendocrine Tumours*; EMA, Ed.; EMA: London, UK, 2016; pp. 1–5.
156. EMA. *Public Summary of Opinion on Orphan Designation; Fosbretabulin Tromethamine for the Treatment of Ovarian Cancer*; EMA, Ed.; EMA: London, UK, 2013; pp. 1–4.
157. Therepetics, M. Developing Innovative Therapeutic Approaches to Treat Cancer; Oxi4503. Available online: <http://www.mateon.com/product-development/taboxi4503/> (accessed on 28 October 2019).
158. Kim, T.J.; Ravoori, M.; Landen, C.N.; Kamat, A.A.; Han, L.Y.; Lu, C.; Lin, Y.G.; Merritt, W.M.; Jennings, N.; Spannuth, W.A.; et al. Antitumor and Antivascular Effects of Ave8062 in Ovarian Carcinoma. *Cancer Res.* **2007**, *67*, 9337–9345. [[CrossRef](#)]
159. Morinaga, Y.; Suga, Y.; Ehara, S.; Harada, K.; Nihei, Y.; Suzuki, M. Combination Effect of Ac-7700, a Novel Combretastatin a-4 Derivative, and Cisplatin against Murine and Human Tumors in Vivo. *Cancer Sci.* **2003**, *94*, 200–204. [[CrossRef](#)]
160. Blay, J.-Y.; Pápai, Z.; Tolcher, A.W.; Italiano, A.; Cupissol, D.; López-Pousa, A.; Chawla, S.P.; Bompas, E.; Babovic, N.; Penel, N.; et al. Ombrabulin Plus Cisplatin Versus Placebo Plus Cisplatin in Patients with Advanced Soft-Tissue Sarcomas after Failure of Anthracycline and Ifosfamide Chemotherapy: A Randomised, Double-Blind, Placebo-Controlled, Phase 3 Trial. *Lancet Oncol.* **2015**, *16*, 531–540. [[CrossRef](#)]
161. Munshi, N.; Jeay, S.; Li, Y.; Chen, C.-R.; France, D.S.; Ashwell, M.A.; Hill, J.; Moussa, M.M.; Leggett, D.S.; Li, C.J. Arq 197, a Novel and Selective Inhibitor of the Human C-Met Receptor Tyrosine Kinase with Antitumor Activity. *Mol. Cancer Ther.* **2010**, *9*, 1544–1553. [[CrossRef](#)]
162. Graveel, C.R.; Tolbert, D.; Vande Woude, G.F. Met: A Critical Player in Tumorigenesis and Therapeutic Target. *Cold Spring Harb. Perspect. Biol.* **2013**, *5*, a009209. [[CrossRef](#)] [[PubMed](#)]
163. Aoyama, A.; Katayama, R.; Oh-hara, T.; Sato, S.; Okuno, Y.; Fujita, N. Tivantinib (Arq 197) Exhibits Antitumor Activity by Directly Interacting with Tubulin and Overcomes Abc Transporter-Mediated Drug Resistance. *Mol. Cancer Ther.* **2014**, *13*, 2978–2990. [[CrossRef](#)] [[PubMed](#)]

164. Clinicaltrials Gov. Tivantinib: Phase 3. Available online: https://clinicaltrials.gov/ct2/results?term=tivantinib&age_v=&gndr=&type=&rslt=&phase=2&Search=Apply (accessed on 25 November 2019).
165. Cabibbo, G.; Enea, M.; Attanasio, M.; Bruix, J.; Craxi, A.; Camma, C. A Meta-Analysis of Survival Rates of Untreated Patients in Randomized Clinical Trials of Hepatocellular Carcinoma. *Hepatology* **2010**, *51*, 1274–1283. [[CrossRef](#)] [[PubMed](#)]
166. El-Khoueiry, A.B.; Sangro, B.; Yau, T.; Crocenzi, T.S.; Kudo, M.; Hsu, C.; Kim, T.Y.; Choo, S.P.; Trojan, J.; Welling, T.H.R.; et al. Nivolumab in Patients with Advanced Hepatocellular Carcinoma (Checkmate 040): An Open-Label, Non-Comparative, Phase 1/2 Dose Escalation and Expansion Trial. *Lancet* **2017**, *389*, 2492–2502. [[CrossRef](#)]
167. Rimassa, L.; Assenat, E.; Peck-Radosavljevic, M.; Pracht, M.; Zagonel, V.; Mathurin, P.; Rota Caremoli, E.; Porta, C.; Daniele, B.; Bolondi, L.; et al. Tivantinib for Second-Line Treatment of Met-High, Advanced Hepatocellular Carcinoma (Metiv-Hcc): A Final Analysis of a Phase 3, Randomised, Placebo-Controlled Study. *Lancet Oncol.* **2018**, *19*, 682–693. [[CrossRef](#)]
168. KyowaKirin Kyowa Hakko Kirin Announces Discontinuation for Developing Arq 197 (Tivantinib). Available online: https://www.kyowakirin.com/media_center/news_releases/2017/e20171006_01.html (accessed on 25 November 2019).
169. Prior, I.; Lewis, P.; Mattos, C. A Comprehensive Survey of Ras Mutations in Cancer. *Cancer Res.* **2012**, *72*, 2457–2467. [[CrossRef](#)]
170. Beyondspring's Novel Study 103 Phase 3 Design in Nslc Presented at 2019 Iaslc World Conference on Lung Cancer. Available online: <https://www.globenewswire.com/> (accessed on 25 November 2019).
171. An Open-Label Study of Intravenous Bal101553 in Adult Patients with Solid Tumors. Available online: <https://clinicaltrials.gov/ct2/show/record/NCT01397929> (accessed on 20 November 2019).
172. Calvert, A.H.; Gonzalez, M.; Ganguli, S.; Ng, M.; Benafif, S.; Capelan, M.; Goldstein, R.; Shah, K.; Jarvis, C.; Flynn, M.; et al. A First-in-Human (Fih) Dose-Escalation Study of the Safety, Pharmacokinetics (Pk), and Pharmacodynamics (Pd) of Intravenous Bal101553, a Novel Microtubule Inhibitor, in Adult Patients with Advanced Solid Tumors. *J. Clin. Oncol.* **2013**, *31*, 2566.
173. Kolb, E.A.; Gorlick, R.; Keir, S.T.; Maris, J.M.; Kang, M.H.; Reynolds, C.P.; Lock, R.B.; Carol, H.; Wu, J.; Kurmasheva, R.T.; et al. Initial Testing (Stage 1) of Bal101553, a Novel Tubulin Binding Agent, by the Pediatric Preclinical Testing Program. *Pediatr. Blood Cancer* **2015**, *62*, 1106–1109. [[CrossRef](#)]
174. Lisavanbulin and Radiation Therapy in Treating Patients with Newly Diagnosed Glioblastoma. Available online: <https://www.cancer.gov/about-cancer/treatment/clinical-trials/search/v?id=NCI-2016-01847&r=1> (accessed on 18 December 2019).
175. Clinicaltrials Gov. A Phase 1/11 Trial of Crolibulin (Epc2407) Plus Cisplatin in Adults with Solid Tumors with a Focus on Anaplastic Thyroid Cancer (Atc). Available online: <https://clinicaltrials.gov/ct2/show/NCT01240590> (accessed on 18 December 2019).



© 2020 by the authors. Licensee MDPI, Basel, Switzerland. This article is an open access article distributed under the terms and conditions of the Creative Commons Attribution (CC BY) license (<http://creativecommons.org/licenses/by/4.0/>).